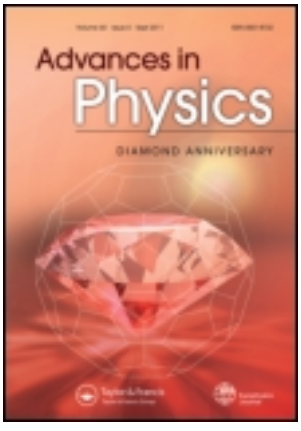

Advances in Physics
Publication details, including instructions for authors and subscription information:
http://www.tandfonline.com/loi/tadp20

Ferroelectric polymers

R.G. Kepler [a] & R.A. Anderson [a]
[a] Sandia National Laboratories, Organization 1800, P.O. Box 5800, Albuquerque, NM, 87185, USA

Version of record first published: 28 Jul 2006

To cite this article: R.G. Kepler & R.A. Anderson (1992): Ferroelectric polymers, Advances in Physics, 41:1, 1-57

To link to this article: http://dx.doi.org/10.1080/00018739200101463

ADVANCES IN PHYSICS, 1992, VOL. 41, NO. 1, 1–57

Ferroelectric polymers

By R. G. KEPLER and R. A. ANDERSON
Sandia National Laboratories, Organization 1800,
P.O. Box 5800, Albuquerque, NM 87185, USA

[Received 3 September 1991]

Abstract

In the early 1970s it became clear that the polymer polyvinylidene fluoride is ferroelectric. There have been extensive studies of its properties and of the properties of copolymers of vinylidene fluoride with tri- or tetra-fluoroethylene. This work has led to a fairly complete understanding of the ferroelectric and related properties of these materials. The emphasis in this review is on the studies of these materials that are oriented toward showing that the polymers are indeed ferroelectric, determining the mechanism of polarization reversal, and understanding the origins of the observed piezoelectric and pyroelectric effects. Very recently some odd nylons (nylons with an odd number of carbon atoms in the monomer unit) were recognized to be ferroelectric, and ferroelectric liquid-crystalline polymers have been prepared by attaching ferroelectric liquid-crystal molecules as side chains to polymer backbones. These new findings are included in the review.

Contents

0001–8732/92 $5·00

1. Introduction

During the 1970s it was discovered that the polymer poly(vinylidene fluoride) (PVF_2) is ferroelectric. PVF_2 has been known since the 1940s and is used extensively as a base for durable long-life coatings for exterior finishes, as an electrical insulator and as a chemically inert material for use in chemical processing equipment. It has a simple chemical structure; with a repeat unit of $-CH_2-CF_2-$, and PVF_2 is readily produced in a flexible thin-film form. The combination of ferroelectricity and these desirable mechanical properties has led to investigations of many possible applications, some of which have been commercialized. Since 1980 there have been over 2000 publications concerning PVF_2 and the vast majority of these are related in some way to the fact that it is ferroelectric.

The discovery of ferroelectricity in polymers actually began as searches for electrets, materials in which an effective macroscopic separation of positive and negative charges can be produced by the application of an electric field. In 1892, Heaviside [1] introduced the term electret by analogy with magnet. The first systematic study of the properties of electrets was undertaken by the Japanese physicist Eguchi in 1919. He prepared electrets from mixtures of beeswax and rosin and produced the macroscopic separation of charge by applying an electric field to the melted mixture and then cooling to solidify [2, 3]. Since those early days, Japanese scientists have devoted considerable effort to studies of the properties of electrets and of materials than might be made into electrets and they very quickly took advantage of those properties. During the Second World War they recognized the potential of electret microphones and used them in the field.

Fukuda [4], among others, has devoted considerable effort to studies of the phenomena of piezoelectricity in biological and polymeric materials. As will be discussed later in this review, some types of electrets exhibit piezoelectricity and it was during a survey of the piezoelectric properties of a wide variety of polymeric materials by Kawai [5] that the unusually large piezoelectric coefficient of PVF_2 was discovered. For the survey, polymeric materials were typically heated to some elevated temperature, an electric field was applied and the sample temperature was lowered in the presence of the field. In these early studies it was recognized that piezoelectricity resulted from oriented dipoles but there was confusion about the role of space charge. Clearly, the procedure used to prepare the samples could produce both oriented dipoles and space charge and many of the early papers attempted to separate the contributions of each.

Bergman and co-workers [6–8] were the first to speculate on the possibility that PVF_2 was ferroelectric. The crystal structure had been studied by Lando *et al.* [9] and one of its polymorphs was known to be polar. In a series of papers, Bergman and co-workers [6–8] reported that PVF_2 was pyroelectric as well as piezoelectric and that it could be used to frequency double neodymium-doped yttrium aluminium garnet laser light. They pointed out these observations were consistent with the hypothesis that PVF_2 was ferroelectric.

It is important at this point to discuss the definitions of ferroelectric and electret because there have been some inconsistences or disagreements regarding usage of the

terms, particularly with regard to PVF_2. Lines and Glass [10] in their book state that, 'Generally speaking electret is used to describe any material in which a polarization persists after the application of an electric field.' Sessler [11] defines an electret as 'a piece of dielectric material exhibiting a quasi-permanent electrical charge. The term "quasi-permanent" means that the time constants characteristic for the decay of the charge are much longer than the time periods over which studies are performed with the electret'. Ferroelectrics on the other hand are defined as materials in which the unit cell of the crystal is polar and the direction of polarization can be changed by the application of an electric field [10, 12]. These definitions suggest that ferroelectrics are a subset of electrets. However, until PVF_2 was fabricated electrets were generally considered to be non-equilibrium materials and, if they were crystalline, the polarization arose not from a polar crystal structure but from trapped charge. Because the discovery that PVF_2 is ferroelectric resulted from studies of electrets and much of the early work emphasized electret-like properties, some workers continue to refer to PVF_2 as an electret, incorrectly in our opinion. We believe that electret should refer only to non-equilibrium materials.

In this review we shall limit our discussions to those polymers which are crystalline with polar unit cells and in which the direction of polarization can be changed by the application of an electric field. The vast majority of the review will be devoted to PVF_2 and its copolymers but some space will be devoted to the new and growing areas of ferroelectric liquid-crystalline polymers and odd nylons. We have not attempted to be comprehensive in this review but have attempted to emphasize those aspects of the physical properties of ferroelectric polymers that we believe would be of most interest to physicists.

A number of reviews have already been written covering various aspects of piezoelectricity, pyroelectricity and ferroelectricity in polymers. Lovinger [13] has published a very thorough review of studies of the crystal structures of PVF_2 and its copolymers and how they are formed and interrelated, and an entire book [14] has been devoted to reviews of the many possible applications of PVF_2 and its copolymers. Other reviews that have been published recently include those by Furukawa [15, 16], Broadhurst and Davis [17] and Davis [18]. The first review relevant to the ferroelectric properties of polymers was published by Hayakawa and Wada [19] and the present authors previously reviewed piezoelectricity and related phenomena in polymers in 1980 [20].

The outline of this review is as follows. Most of the review will be devoted to PVF_2 and its copolymers and that subject will be covered starting in the next section. The molecule, crystal structure and morphology will be covered first, followed by major sections on ferroelectric, pyroelectric and piezoelectric properties. In the section on ferroelectric properties, considerable space is devoted to the extensive evidence that PVF_2 and its copolymers are indeed ferroelectric. In the sections on pyroelectricity and piezoelectricity experiments directed towards determining the basic mechanisms involved and theoretical models are emphasized. The section on PVF_2 and its copolymers is followed by a short section on other ferroelectric polymers and a section containing concluding remarks.

2. Poly(vinylidene fluoride) and its copolymers

2.1. *The poly(vinylidene fluoride) molecule*

PVF_2 has the relatively simple molecular structure $(CF_2CH_2)_n$ where n is typically greater than 10000. A perfect molecule would have all the carbon atoms bonded to

hydrogen atoms attached only to carbon atoms bonded to fluorine atoms. When the molecules are synthesized, a certain fraction of the monomer units (CH_2CF_2), are reversed, creating what are called head-to-head (HH) or tail-to-tail (TT) defects. It has been found that, during synthesis, one defect immediately follows the opposite kind of defect creating a pair, head-to-head and tail-to-tail (HHTT) [21]. The concentration of these defects depends on the synthesis conditions and plays an important role in the physical properties of the materials prepared.

No attempt will be made to discuss the synthesis of the molecules in this paper. Readers interested in the synthesis are referred to the review by Lovinger [13]. Typical molecular weights of commercially available polymers are from 2×10^6 to 5×10^6 or approximately 30 000 to 80 000 monomer units per chain [13].

Farmer *et al.* [22] have investigated theoretically the effect of the concentration of defects on the potential energy of two different conformations of the polymer. In their theory they included both steric and electrostatic effects. They numerically calculated the steric potential energy using the potential functions proposed by DeSantis *et al.* [23]. The electrostatic energy was calculated by assuming that each atom was charged and summing pairwise over the atoms.

The molecular conformations considered were all-*trans* (TT) and *trans–gauche–trans–gauche'* (TGT$\bar{\text{G}}$). Pictures of space-filling models in these conformations and in a third, T3GT3$\bar{\text{G}}$ (all three of which are observed in the crystal polymorphs to be discussed later) are shown in figure 1, together with schematic representations of the view parallel to the chain axis in each of the conformations. The two conformations

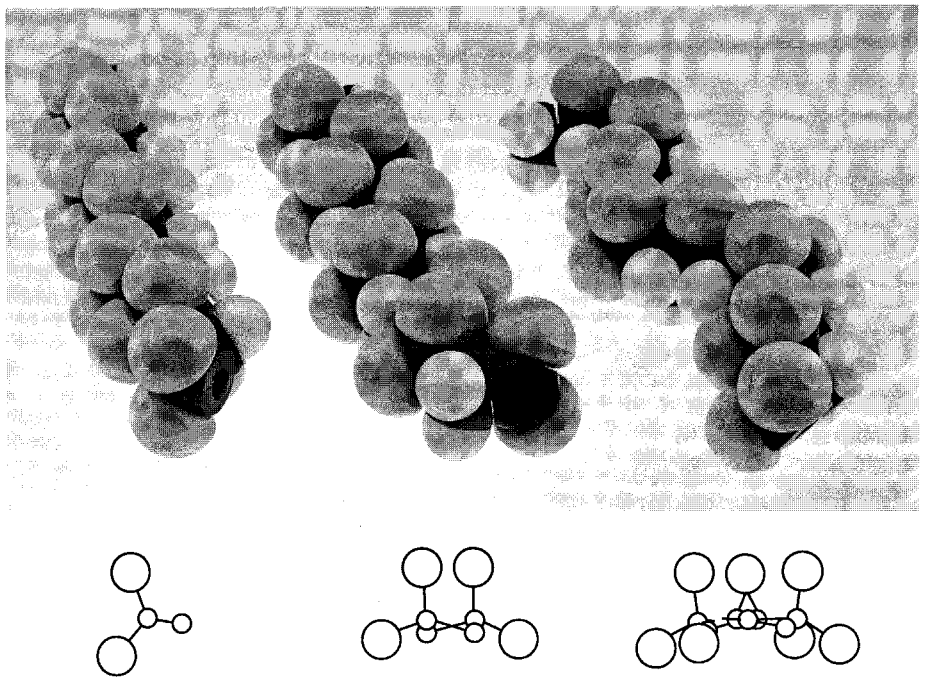

Figure 1. A photograph of space-filling models of the three PVF_2 molecular conformations, all *trans*, TGT$\bar{\text{G}}$ and $T_3GT_3\bar{G}$ going from left to right, as determined from X-ray crystal structure analyses. The pictorial representations at the bottom indicate a view parallel to the chain axis, where the large circles are for fluorine atoms and small circles for carbon atoms. The hydrogen atoms were left out for clarity.

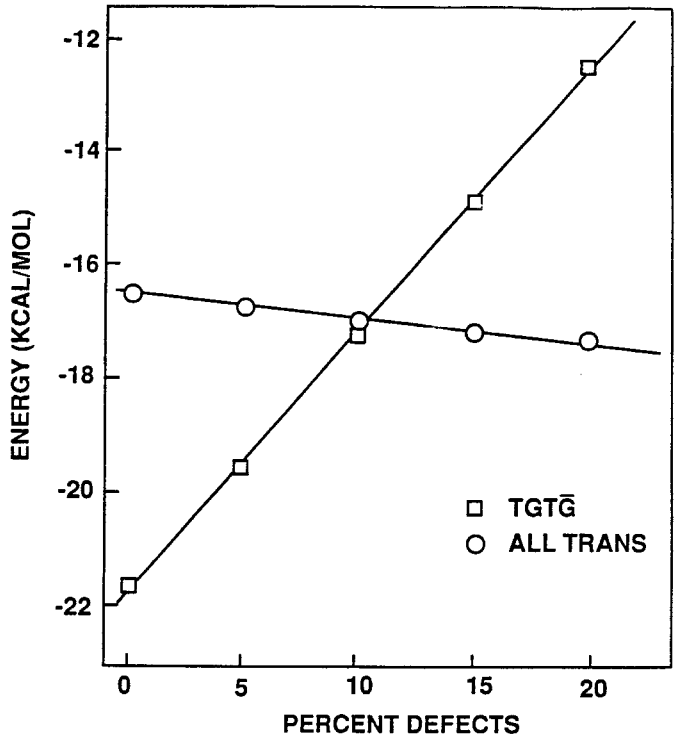

Figure 2. Potential energy of all-*trans* (○) and TGTḠ (□) chain conformations plotted against HHTT defect density as calculated by Farmer *et al.* [22].

chosen are the most common observed in crystals as determined by X-ray crystal structure investigations. The calculated potential energies of the two chain conformations as a function of defect density are shown in figure 2. It was found that at low defect concentrations the TGTḠ conformation was the most stable but that at high defect concentrations the all-*trans* conformation was most stable. The cross-over point was predicted to be about 11% defects. As will be discussed in the next section, recent crystal structure studies of the effect of defects tend to support this conclusion.

Random copolymers of vinylidene fluoride (VDF) and trifluoroethylene (F_3E) or tetrafluorethylene (F_4E) have also been synthesized. The randomly distributed F_3E and F_4E monomer units appear to play a similar role to that of the HHTT defects. Their presence stabilizes the all-*trans* conformation and produces some very interesting new materials as will be discusssed later. Farmer *et al.* [22] studied the effect of F_4E monomers using the theory mentioned above and predicted that their presence should stabilize the all-*trans* conformation at a concentration which was in qualitative agreement with experimental results of Lando and Doll [24].

2.2. *Crystal structure and morphology*

PVF_2 is a crystalline polymer, which means that in some regions the molecules are arranged in a regular array. Various types of estimates lead to the conclusion that about one half of the volume of PVF_2 consists of these organized regions [25].

Crystal structures of PVF_2 have been the subject of many investigations and a very thorough review has been written by Lovinger [13]. One reason that PVF_2 has been

studied so intensively is that it has at least four polymorphs and, as soon as it was found to exhibit interesting electrical properties which were related to the crystal structures, studies of the crystal structure intensified. The large number of studies has led to considerable nomenclature confusion. We shall follow the recommendations of Lovinger [13] and use Greek letters to refer to the four well-established polymorphs. The most commonly observed structure, obtained primarily by quenching from the melt, is the non-polar α-phase or phase II. The phase of most interest for electrical properties is the ferroelectric β-phase (phase I). The other two forms we shall refer to as the γ- and δ-phases, frequently referred to as phases III and IV respectively. Both of these forms are also polar but the unit-cell dipole moment is smaller than that in the β-phase and they have not been subjected to intensive electrical investigations. Two other polymorphs have been identified or suggested [26, 27] but will not be discussed.

The crystal structure for the non-polar α-phase is shown in figure 3. Lando *et al.* [9] were the first to assign the correct unit-cell dimensions, but several subsequent studies were required to sort out the correct crystal structure [28–30]. The molecules are in a distorted TGTḠ conformation [29] and that conformation has a net dipole moment. However, there are two molecules per unit cell and the dipole moment of the two molecules are oriented in opposite directions.

The structure of most interest for its electrical properties is the β-phase shown in figure 4. This structure has been studied by Gal'perin *et al.* [31], Lando *et al.* [9] and Hasegawa *et al.* [29]. The molecule is in the all-*trans* conformation, which exhibits the largest dipole moment, and the dipole moment of the two molecules in the unit cell are oriented in the same direction. The fluorine atoms are too large to allow a simple all-*trans* conformation and it is believed that they are statistically offset as depicted by

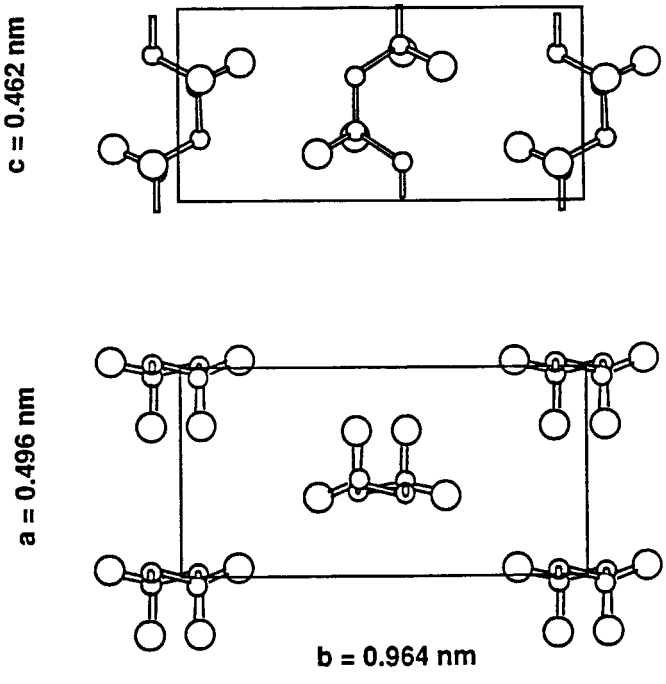

Figure 3. Crystal structure of the non-polar α-phase of PVF_2. (Adapted from Hasegawa *et al.* [29].)

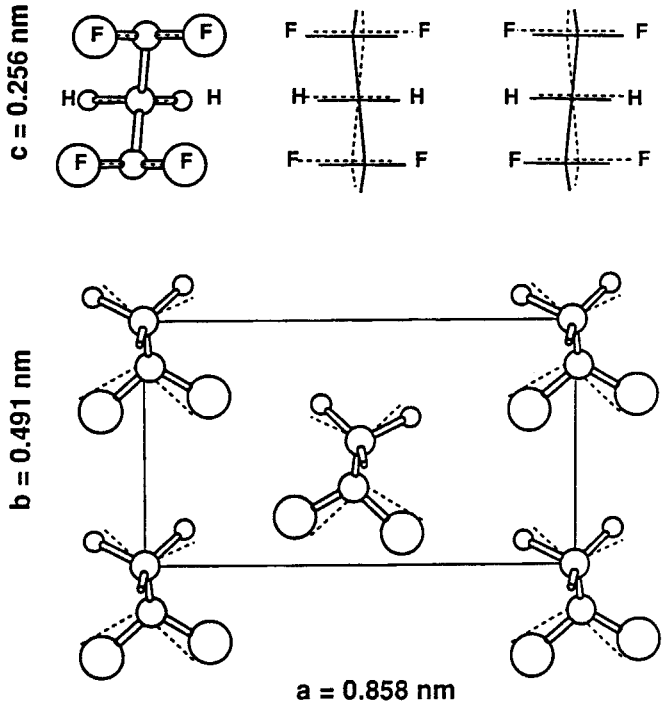

Figure 4. Crystal structure of the polar β-phase of PVF_2. (Adapted from Hasagawa *et al.* [29].)

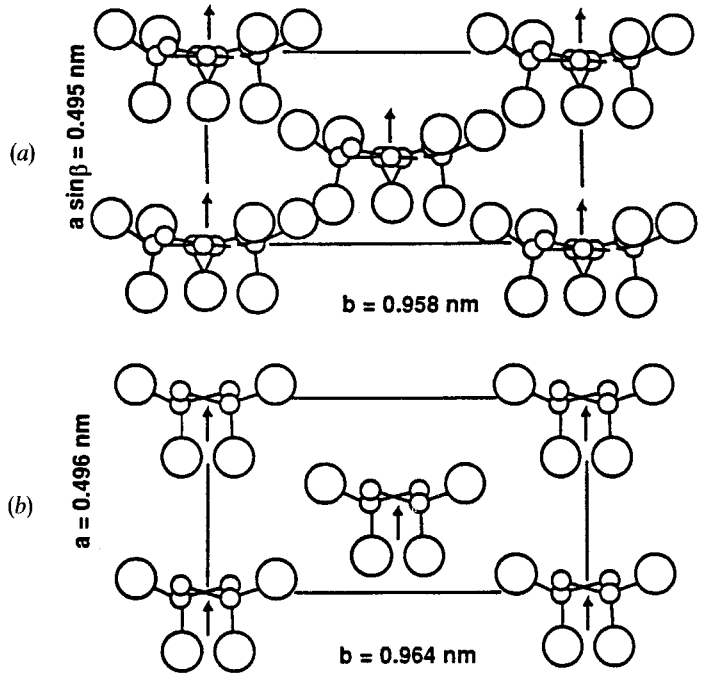

Figure 5. Schematic diagram of the molecular orientations in (*a*) the γ-phase and (*b*) the δ-phase.

broken lines in figure 4. This phase is typically obtained by drawing α-phase films to several times their initial length, a process which produces highly oriented β films with a chain axis parallel to the draw direction.

The polar γ- and δ-phase crystal structures are shown schematically in figure 5. The molecular conformation in the δ-phase (TGTḠ) is the same as that in the α-phase but the dipole moments of the two molecules in the unit cell are aligned, providing a polar crystal [32, 33]. This phase can be obtained by applying a high field to an α-phase film [32]. In the γ-phase the molecules are in the $T_3GT_3\bar{G}$ conformation with two molecules per unit cell and with the dipole moments aligned [34–36].

As might be expected, the interrelation among these various phases is quite complex [13]. The phases and transformations between the phases can be produced by a variety of means and a summary, as provided by Lovinger [13], is shown in figure 6. When crystalline polymers crystallize, the polymer molecules typically form lamellae of the order of 10 nm thick and the lamellae form spherulites. The polymer molecules are oriented perpendicular to the surface of the lamellae and are folded in such a way as to penetrate the lamellae many times. A schematic diagram of this morphology is presented in figure 7. In PVF_2, approximately half of the molecules are in the amorphous or non-crystalline phase. For work on the electrical properties, films of this

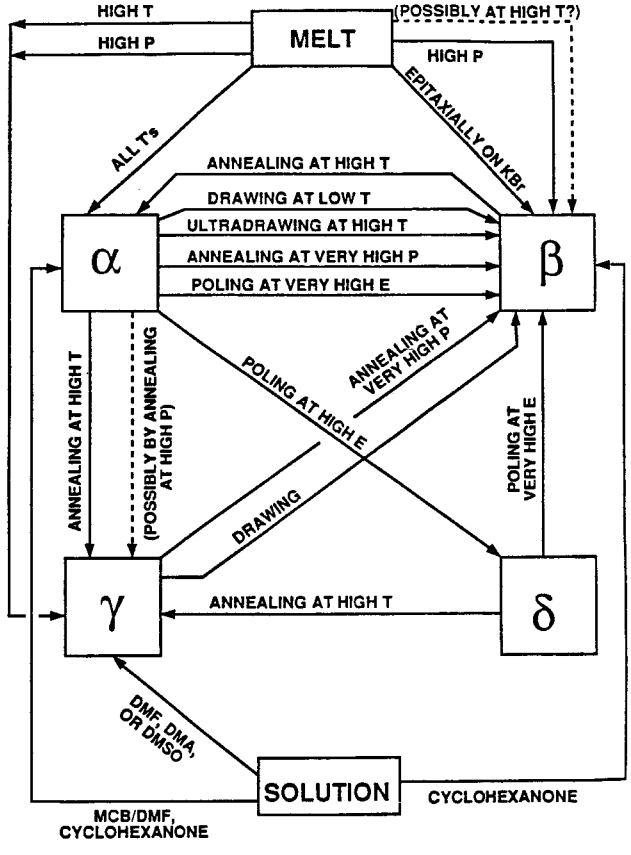

Figure 6. The interrelations between the four well established phases of PVF_2: DMF, dimethylformamide; DMA, dimethylacetamide; DMSO, dimethyl sulphoxide; MCB, monochlorobenzene. (From Lovinger [13].)

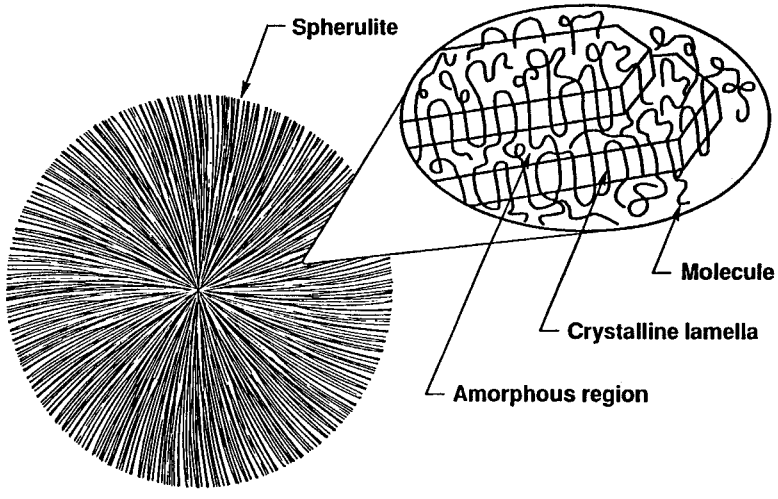

Figure 7. Schematic diagram of the spherulitic morphology of semicrystalline polymers. (Adapted from Broadhurst and Davis [17] and Lovinger [204].)

morphology and in the α-phase are stretched to several times their original length and in the process the lamellae are oriented perpendicular to the draw direction so that the molecules are parallel to the draw direction [9, 37], and the phase changes to β.

Cais and Kometani [38] have synthesized PVF_2 molecules with defect concentrations ranging from 0·2 to 23·5 mol% and their effect on the crystal structures obtained has been studied [39]. It was found that below a defect concentration of about 11 mol% the α-phase was obtained by quenching from the melt while above that concentration the β-phase was obtained as predicted by Farmer *et al.* [22]. Lando and Doll [24], in an earlier attempt to simulate the effect of HHTT defects and to test the predictions of Farmer *et al.* [22], synthesized random copolymers of VDF and F_4E and found, in agreement with the predictions, that below a concentration of about 7 mol% F_4E the α-phase was formed. As we shall discuss later, these defects also have a marked effect on the ferroelectric properties of the polymers and have made it possible to study ferroelectric-to-paraelectric transitions in these materials.

Ohigashi and co-workers [40, 41] have studied the growth of crystals in samples of both VDF–F_3E and PVF_2. They have grown lamellar crystals of PVF_2 0·2 μm thick and 10 μm wide in material subjected simultaneously to a high temperature and a high pressure.

2.3. *Ferroelectricity*

2.3.1. *Proof of ferroelectricity*

Interest in the electrical properties of PVF_2 began in 1969 when Kawai [5] showed that thin films that had been poled exhibited a very large piezoelectric coefficient, 6·7 pC N^{-1}, a value which was about ten times larger than he had found in any other polymer. Poling at that time consisted typically of heating a film above a temperature of about 100°C and applying a high electric field, typically above 50 MV m^{-1}. A short time later, Bergman and co-workers in a series of papers [6–8] reported that PVF_2 was pyroelectric and that thin films could be used to double neodymium laser light. They also speculated on the possibility that PVF_2 was ferroelectric. It was known that the β-phase was polar and would be pyroelectric but it was not known what the poling process was orienting in the partially crystalline film. It was possible that molecular

dipoles in the amorphous phase were being oriented by the field at high temperatures and that the orientation was locked in when the temperature was lowered. This hypothesis seemed unlikely, however, since the glass transition temperature of the amorphous phase is about −40°C. Since the definition of a ferroelectric crystal is that it has a polar unit cell and that a high electric field can change the orientation of the dipole moment, it was necessary to show that the dipoles in the crystalline phase of PVF_2 were being reoriented.

In an attempt to show that the dipoles in the crystalline phase were being reoriented, Kepler and Anderson [42] measured the intensity of Cu Kα X-rays diffracted from β-phase films at an angle 2Θ of 20·7° as a function of the sample orientation. They showed that the results from poled and unpoled films were different. At $2\Theta = 20{\cdot}7°$ the X-rays are diffracted from the 110 and 200 planes. The samples were mounted with an axis of rotation in the plane defined by the incoming and outgoing diffracted X-ray beam and the intensity of the diffracted beam was measured as the sample was rotated about that axis. The most significant results were obtained when the axis of rotation coincided with the sample draw direction. In the β-phase prepared by drawing, the molecular chain axis coincides with the draw direction and the dipole moments are perpendicular to the draw direction. The results are shown in figure 8.

It is of interest to point out that, if the electric field simply flipped the orientation of the dipoles by 180°, only an extremely small change in the diffracted X-ray intensity would have been observed. Kepler and Anderson [42] interpreted their results by pointing out that, even though the β-phase unit cell is orthorhombic, it is very close to being hexagonal. Only a 1% distortion of a primitive hexagonal lattice is required to produce the β-phase unit cell. Therefore rotation of the dipole moments of the unit cell

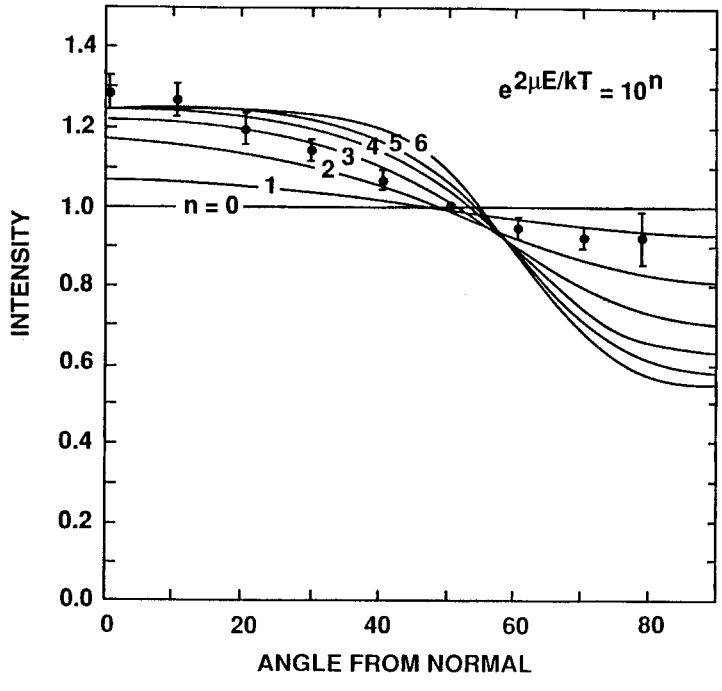

Figure 8. Comparison of X-ray diffraction intensity measurements with a simple model. (From Kepler and Anderson [42].)

could be accomplished in 60° increments by rotating each chain 60° without disrupting the crystal morphology. The theoretical curves shown in figure 8 were obtained by assuming that the rotatable units had a dipole moment μ which was perpendicular to the draw direction and randomly oriented in that plane and that under the applied field they assumed an equilibrium distribution constrained by rotations in 60° increments.

Takahashi and Odajima [43] have conducted a more thorough X-ray investigation of crystallite reorientation during the poling process and concluded that their results were consistent with the 60° increment model also. Takahashi *et al.* [44] have also observed the few per cent change in intensity of the diffracted X-rays expected in a polar crystal when the direction of polarization is changed by 180°, providing direct evidence for a reversal in direction of polarization by an applied electric field.

Perhaps the most interesting X-ray diffraction demonstration of the 60° increment model is that of Bur *et al.* [45]. They used films 1 mm thick which had been simultaneously rolled (to stretch and convert α-phase material to β-phase) and poled [46]. Rolling produces a material with a single-crystal-like texture with the *c* axis parallel to the direction of rolling, the *a* axis perpendicular to the film surface and the *b* axis parallel to the film surface [46]. Bur *et al.* [45] prepared a cylinder 1 mm in diameter, machined from a single sheet 1 mm thick, with the axis of the cylinder parallel to the rolling or stretch direction and studied the intensity of X-rays diffracted at $2\Theta = 20{\cdot}7°$ as a function of the angle of rotation as the cylinder was rotated about its axis. The results expected for an unpoled sample and for unit cells rotated by 60° from the unpoled orientation are shown in figure 9 and experimental results obtained for an 'unpoled' sample and a poled sample are shown in figures 10(*a*) and (*b*) respectively. The 'unpoled' sample was one which had been initially poled and then subjected to a temperature cycle in which it was heated to 152°C, held at that temperature for 10 min and then cooled to room temperature. It is easy to see that the experimental results for the 'unpoled' sample in figure 10(*a*) corresponds to figure 9(*a*) and that the results for a poled sample in figure 10(*b*) corresponds to the sum of figures 9(*b*) and (*c*). The solid

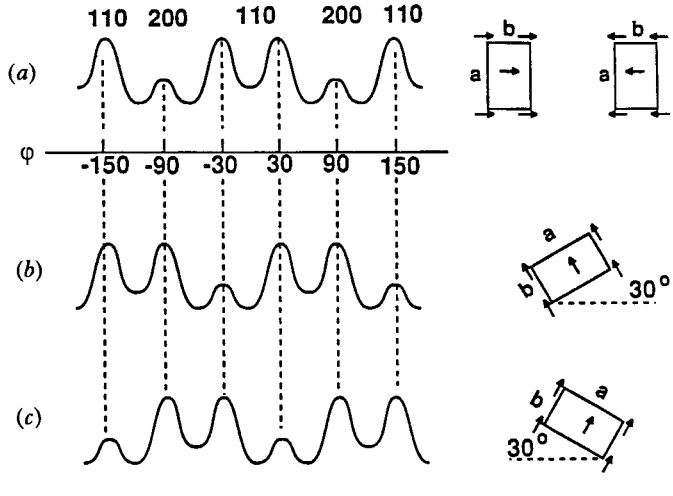

Figure 9. Diffracted X-ray intensity expected against angle of rotation for (*a*) an unpoled sample with a single-crystal texture, (*b*) a sample in which the unit-cell *b* axis has been rotated 60° clockwise and (*c*) a sample in which the unit-cell axis has been rotated 60° counterclockwise.

curve in figure 10 (*b*) was obtained from a mathematical model of the intensity against ϕ curves for different crystal orientations in the form of the von Mises equation [47]

$$I(\phi)=CD(\rho)\sum_{i=1}^{6}A_i\exp\{\rho[\cos(\phi-\phi_i)-1]\}, \tag{1}$$

where

$$\phi_i=\phi_0+60i-210, \tag{2}$$

$$A_1=A_3=A_4=A_6=\frac{P}{4}+f\left(1-\frac{P}{2}\right). \tag{3}$$

and

$$A_2=A_5=\frac{(1-P)}{2}+fP. \tag{4}$$

P is the fraction of (200) plane normals that are aligned in directions other than normal to the film surface ($i=1,3,4,6$) and $f=(S_{110}/S_{200})^2$ where S_{hkl} is the structure factor for the *hkl* reflection, $D(\rho)$ is a normalization constant chosen so that

$$1=D(\rho)\int_{-\pi}^{\pi}\exp[\rho(\cos\phi-1)]\,\mathrm{d}\phi \tag{5}$$

and C is a scaling factor. More will be said about these results later.

Tamura *et al.* [48] and Naegele and Yoon [49] have studied the effect of the poling process on the infrared absorption spectrum of β-phase PVF_2 and showed that their results were consistent with an electric field reorientation of the direction of polarization of the crystalline phase. They measured the effect of an electric field on absorption at 512 and 446 cm^{-1}. These absorptions occur in the β-phase with their transition moments oriented perpendicular to the chain axis. The transition moment at 512 cm^{-1} is parallel to the CF_2 dipole moment and the transition at 446 cm^{-1} perpendicular to it [50, 51]. The percentage transmission at 512 cm^{-1} as a function of the applied field strength obtained by Naegele and Yoon [49] is shown in figure 11. It is seen that, as the field strength is reduced from a value high enough to polarize the sample, the transmission decreases and, as the field direction is reversed and increased in magnitude, the transmission goes through a minimum and finally returns to the original value as the magnitude of the field becomes large enough to reverse the polarization. At 412 cm^{-1} the behaviour of the transmission is just the opposite. The transmission first increases and then decreases. These results showed that during the poling process the orientation of the dipole moments in the β-phase was being changed and that they were not simply flipping by 180°. They had to be going through intermediate orientation states that led to increased or decreased transmission.

Aslaksen (52) was the first to attempt a theoretical model of ferroelectricity in PVF_2 and he assumed that the chains would rotate by 180°. Dvey-Aharon *et al.* [53] have undertaken a detailed theoretical examination of polarization reversal in PVF_2 and have concluded that it cannot occur by a 180° rotation of the chain segments but that it can occur in 60° increments. For the 180° model they started with phenomenological Hamiltonian of the form $H=T+V$ where

$$T=\tfrac{1}{2}I\sum_i\dot{\theta}_i^2 \tag{6}$$

and

$$U=\sum_i\{A_1[1-\cos(\theta_i)]+A_2[1-\cos(2\theta_i)] \tag{7}$$

$$+\tfrac{1}{2}k(\theta_i-\theta_{i+1})^2\}, \tag{8}$$

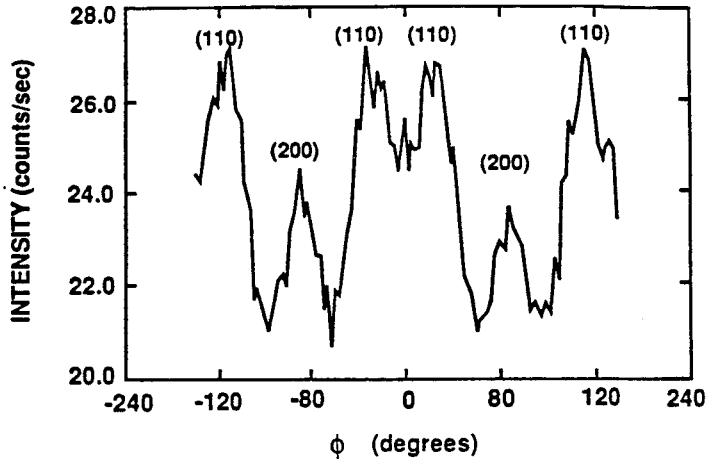

(*a*)

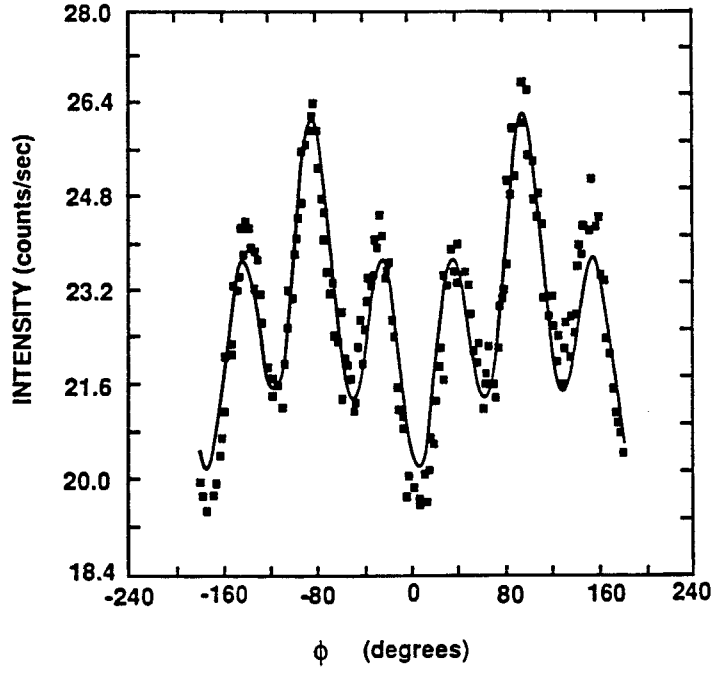

(*b*)

Figure 10. Intensity of X-rays diffracted from a cylindrical sample machined from a rolled film of PVF_2 1 mm thick: (*a*) data obtained on a sample which had been initially poled and subsequently heated to 152°C for 10 min to unpole it; (*b*) data obtained on a poled sample. (From Bur *et al.* [45].)

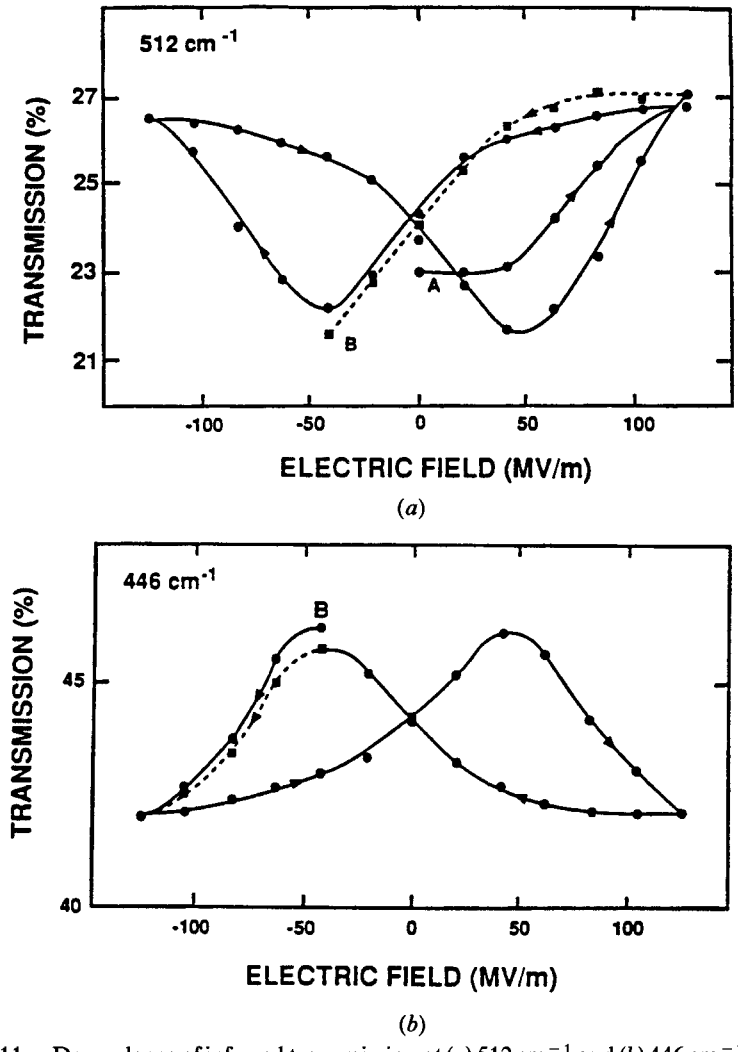

Figure 11. Dependence of infrared transmission at (*a*) 512 cm^{-1} and (*b*) 446 cm^{-1} on an applied electric field. The field was varied in steps of 210 kV cm^{-1} at an interval of 2 min after each increase. An unpoled sample was introduced at point A and the field was varied in the direction indicated by the arrows. The point B in (*a*) is the same as that in (*b*) and is the point at which the wavelength was changed (From Naegele and Yoon [49].)

where θ_i is the angle of rotation of CF_2–CH_2 units from the plane of the crystalline b axis, the dot signifies differentiation with respect to time and I is the moment of inertia of a monomer unit about the centre-of-mass axis of the chain. The first two terms in U represent the interchain and electric field forces on a monomer unit and the third is the torsional rigidity of the chain. A_1 consists of two terms: one which depends on the orientation Δ of neighbouring chains and one which depends on the product of the applied field E and the dipole moment p of the monomer unit. Thus $A_1 = \Delta - pE$. For it to be energetically favourable for a chain to rotate by 180° in this model the applied field must be greater than Δ/p. Dvey-Aharon *et al.* [53] estimated, using a number of experimentally determined constants, that it would take an electric field of the order of

ten times greater than used experimentally to meet this criterion for a chain surrounded by like oriented chains and they suggested that it would be possible to reorient only those chains at a domain wall where half the nearest neighbours are oriented parallel to the applied field and half are antiparallel. In that environment, $\Delta = 0$.

The mechanism for chain reorientation which they proposed involves thermally activated formation of kinks in a chain at a lamella surface followed by rapid motion of the kink through the lamella, about 10 nm, if the chain is at a domain wall. They showed that the motion of the kink, a soliton, through the lamella would be rapid compared with the formation time of kinks. For the 180° model they concluded that the waiting time for the formation in kinks was too long to make that model viable.

As an alternative they considered the 60° model proposed by Kepler and Anderson [42] and modified their equations accordingly. The domain wall between two differently oriented regions is shown schematically in figure 12 and their calculated potential energy as a function of rotation angle of the molecule labelled 1 in figure 12 is shown in figure 13. For this model there is an intermediate minimum in the potential at 30°. No equivalent minimum was found for the 180° model and its presence was found to have a marked effect on the probability of formation on kinks. In the 180° model no kink–antikink pairs could form in the interior of a lamella because of the large amount of energy required to form two kinks simultaneously but in the 60° model it was found that the 30° minimum readily traps segments of the chain which subsequently complete the 60° transition. Dvey-Aharon *et al.* [53] estimated that in this model the rotation of a chain would take of the order of 50 ps at 373 K with an electric field of 100 MV m^{-1}. In order to calculate a macroscopic poling time they pointed out that, at a given time, only a few molecules would be in the required environment depicted in figure 12 so that the molecules in a given crystallite would have to reorient essentially sequentially, one

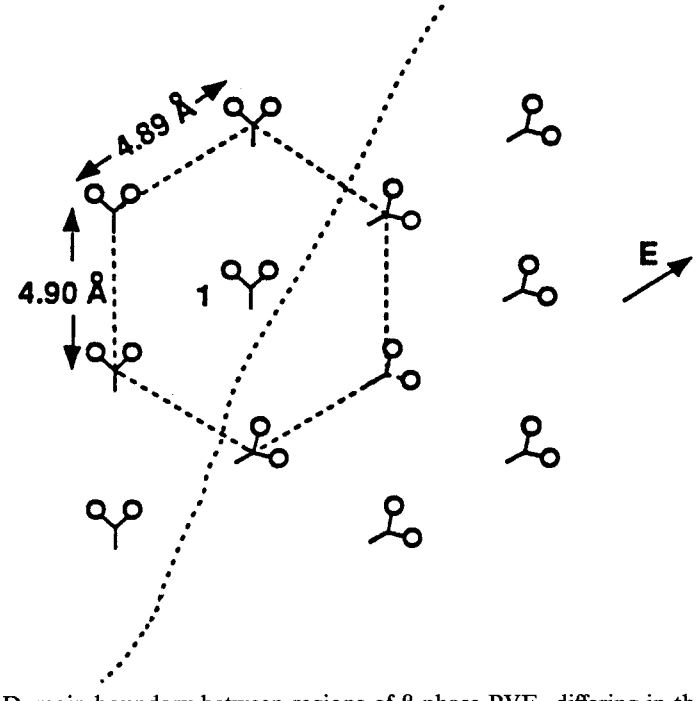

Figure 12. Domain boundary between regions of β-phase PVF_2 differing in the direction of polarization by 60°C. (From Dvey-Aharon *et al.* [53].)

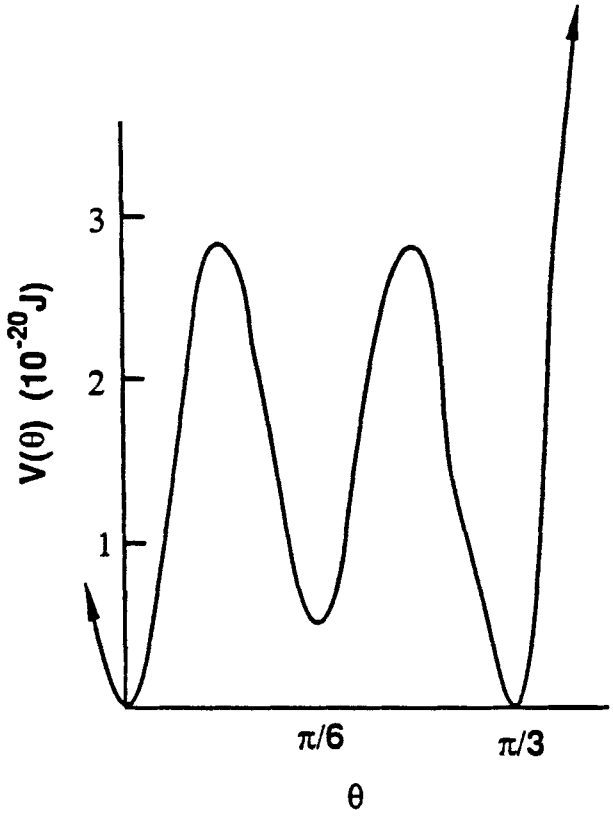

Figure 13. Potential energy against angle θ for the chain labelled 1 in figure 12. The zero of θ is the vertical direction. (From Dvey-Aharon *et al.* [53].)

chain at a time. Since a crystallite probably consists of 10^7 chains, the poling time was predicted to be of the order of 1 ms, much shorter than the estimated poling times, of the order of seconds [54], at the time of publication. More will be said about this issue in section 2.3.3.

To summarize this section, we have presented X-ray and infrared absorption data which show that an applied electric field changes the orientation of the polarization of the crystalline region in PVF_2. Since the definition of a ferroelectric material is one which has a polar unit cell and in which the direction of polarization can be changed by the application of an external field, the data prove that PVF_2 is ferroelectric. These data also show that the reorientation process involves intermediate steps and therefore is not a simple 180° rotation. A 60° rotation model was introduced which is consistent with the experimental observations. A detailed theoretical investigation at the molecular level of the mechanism of molecular reorientation was discussed. The conclusion of this investigation was that reorientation by 180° did not appear to be possible but that reorientation in 60° increments could take place rapidly enough to be consistent with the experimental observations.

2.3.2. *Remanent polarization*

In this section we shall examine the magnitude of the remanent polarization and discuss what can be said about the magnitude of the local field. Hysteresis loops have

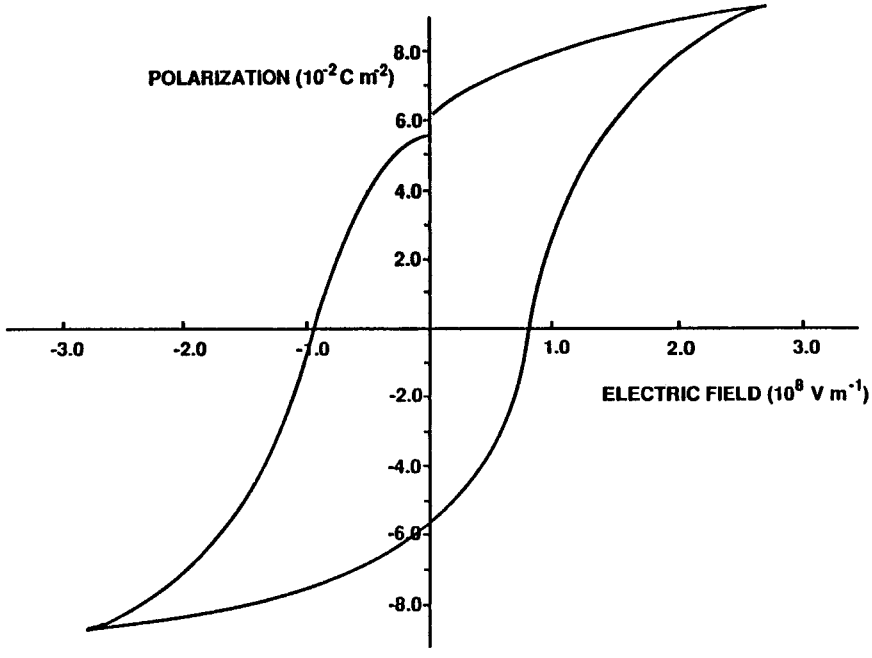

Figure 14. Hysteresis loop obtained on a film of PVF_2 25 μm thick by sweeping the electric field through 1 cycle in a symmetrical triangular wave pattern with a peak height of 280 MV m^{-1} and a period of 30 s. 1 cycle of a series of cycles is shown. (From Kepler [56].)

been measured by many groups, only a few of which are referenced [55–59]. Typical results obtained at room temperature [56] are shown in figure 14. PVF_2 is a good dielectric at room temperature so that conductivity does not interfere appreciably with the acquisition of good hysteresis loops. The data shown in figure 14 were obtained on a poled sample by sweeping the electric field through 1 cycle in a symmetrical triangular wave pattern with a peak height of 280 MV m^{-1} and a period of 30 s. In this study, two types of material were investigated, namely 30 μm uniaxially oriented Piezo Film and 25 μm biaxially oriented capacitor grade film, both of which were obtained from Kureha Chemical Company. Essentially the same hysteresis loops were obtained on the uniaxially oriented films which are essentially all β-phase and on the biaxially oriented films which are approximately half α- and half β-phase. For a sample of ten uniaxially oriented films the average remanent polarization was 0·0583 C m^{-2} with a standard deviation of 0·0027 C m^{-2} and for ten biaxially oriented films the remanent polarization was 0·0633 ± 0·0017 C m^{-2}. The coercive field for both types of sample was found to be about 90 MV m^{-1} but was slightly smaller for the uniaxially oriented film than for the biaxially oriented film.

The remanent polarization of the same 20 samples was also measured by measuring the amount of charge released by the sample when it was suddenly heated to above the melting temperature, about 175°C. The remanent polarization of the ten uniaxially oriented samples obtained this way was 0·0447 ± 0·0028 C m^{-2} and for ten biaxially oriented samples was 0·0565 ± 0·0012 C m^{-2}.

It was initially very surprising that the remanent polarization of the biaxially oriented film was not only as large as, but even larger than, that of the uniaxially oriented film. The crystal structure of the α-phase was known to be non-polar while

that the β-phase was polar. Therefore a film which consisted of half α-phase and half β-phase would be expected to exhibit a smaller remanent polarization than one that was all β-phase. There were other observations that something unusual was happening. Luongo [60] had reported in 1972 that fields of $30\,MV\,m^{-1}$ could convert α-phase material to β-phase and Southgate [61] and Latour [62] reported that, based on infrared spectra, something happened to α-phase material but what was happening was not clear. Das-Gupta and Doughty [63, 64] reported changes in X-ray diffraction peaks which tended to indicate that the amount of α-phase material was reduced by the poling process and Sussnar *et al.* [65] showed that relatively high pyroelectric coefficients are exhibited by samples which, prior to poling, were essentially all α-phase.

Davis *et al.* [32] clarified the situation, as mentioned earlier, when they showed, using X-ray diffraction and infrared absorption, that α-phase material was converted to δ-phase material by electric fields of the order of $120\,MV\,m^{-1}$ and that δ-phase material was converted further to β-phase at higher fields. The conversion from α- to δ-phase involves somehow reversing the orientation of one of the chains in the unit cell so that the dipole moments of the two chains are parallel. A number of workers [32, 66–68] have suggested that this could occur by a simple physical rotation of half the chains by 180°, and Dvey-Aharon *et al.* [69] have considered the possibility that propagation of a 180° kink along half the chains is involved. Lovinger [70] has pointed out that it could occur by what appears to be a simpler mechanism which requires no chain rotation but involves only small intramolecular rotations about all G and $\bar{G}$ bonds of every second chain, causing the conformation to be altered from TGT$\bar{G}$ to T$\bar{G}$TG, thus reversing the direction of the dipole moment but maintaining the overall chain direction. This process is shown schematically in figure 15.

Annealing has been shown to have a large effect on the magnitude of the remanent polarization that can be achieved. Takase *et al.* [71] reported that, by annealing stretch oriented films of PVF_2 close to 180°C prior to poling, this changed the remanent polarization from 0·056 to 0·085 $C\,m^{-2}$, and Ohigashi and Hattori [41] have prepared films by heating them to above 280°C under pressure of 2–5 kbar, with silicone oil as the pressure transmission fluid and have achieved a remanent polarization of 0·1 $C\,m^{-2}$. Bauer [72] reported having achieved a remanent polarization of 0·1 $C\,m^{-2}$ for a biaxially oriented film but no processing conditions were given. Takase *et al.* [73] have found that remanent polarizations of 0·1 $C\,m^{-2}$ can be achieved in deuterated PVF_2 and remanent polarizations of 0·1 $C\,m^{-2}$ are routinely observed in VDF–F_3E copolymers.

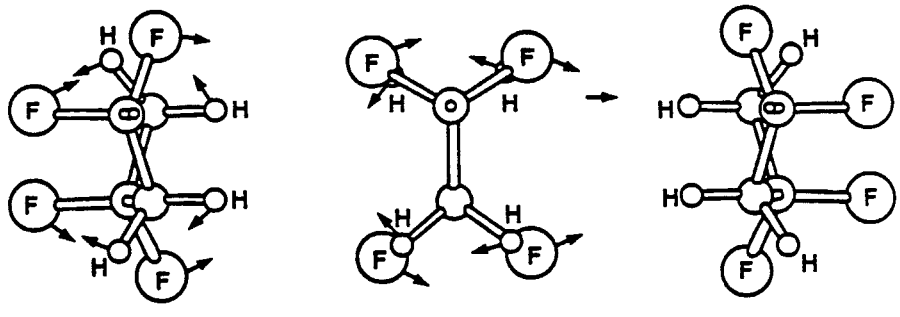

Figure 15. Schematic representation of the intramolecular rotations required in every second polymer chain to transform from the α- to δ-phase (From Lovinger [70].)

The remanent polarization in PVF_2 is only weakly dependent on temperature from 20 to $-100°C$, increasing slightly with decreasing temperature, while the coercive field is a strong function of temperature, increasing from $30\,MV\,m^{-1}$ at 100°C to $180\,MV\,m^{-1}$ at $-100°C$ [57]. Attempts to measure the remanent polarization much above room temperature are plagued by sample conductivity problems.

Bur *et al.* [45], in the work which was introduced in section 2.3.1, carried out careful measurements of the intensity of X-rays diffracted from a cylinder of PVF_2 which had been cut from a poled film 1 mm thick. Fitting their experimental data to the model briefly described previously, they estimated that the remanent polarization of their sample was $0{\cdot}043\,C\,m^{-2}$, somewhat smaller, as expected, than the remanent polarization from hysteresis loops on samples which have not been rolled and thus do not start from the single-crystal texture. By heating the sample to some elevated temperature, holding it at that temperature for 10 min and then lowering the temperature to room temperature before making another X-ray measurement, they studied the stability of the remanent polarization. It was found to be stable up to 75°C and then to decrease linearly with temperature up to 152°C at which point about half the initial polarization was left.

Similar behaviours were observed in pyroelectric coefficient and hydrostatic piezoelectric coefficient measurements on samples of the same material undergoing the same heat treatment. This decrease was attributed to a very broad range of Curie temperatures for the crystalline regions. It was shown that the crystallinity was not changing and other phases were not appearing. However, it seems that the depolarization might arise from crystal melting at the higher temperatures. As Bur *et al.* [45] point out, thermodynamic transformations which occur over a broad temperature range are not uncommon in polymers. If the phase transition involved were a Curie transition, some constraint on the polymer chains would have to orient the dipoles preferentially in the plane of the film as the sample temperature was lowered. It appears equally probable that, if melting were involved, the local stresses developing as the temperature was lowered would lead to the same crystal phase and orientation produced by the processing initially.

In order to calculate what the remanent polarization would be if the crystalline regions were all aligned by an electric field, we note that the dipole moment of a monomer unit in the absence of external fields is $7{\cdot}0 \times 10^{-30}\,C\,m$ [56]. This value is obtained by simply taking a vector sum of the bond dipole moments for the C–F and C–H bonds [74], $4{\cdot}7 \times 10^{-30}$ and $1{\cdot}3 \times 10^{-30}\,C\,m$ respectively, keeping in mind that the carbon end is positive in the C–F bond and negative in the C–H bond. There are two monomer units per orthorhombic unit cell of dimensions $a = 8{\cdot}58$ Å, $b = 4{\cdot}91$ Å and c (chain axis) $= 2{\cdot}56$ Å with their dipole moments parallel to the b axis [29] and the F–C–F and H–C–H bond angles are [29] 108° and 112° respectively. Therefore, if it is assumed that the monomer units are rigid dipoles of dipole moment $7{\cdot}0 \times 10^{-30}\,C\,m$ and that these dipoles are rigidly aligned in crystals, the polarization of a single β-phase crystal of PVF_2 would be $0{\cdot}131\,C\,m^{-2}$. Since PVF_2 samples typically are about 50% crystalline, this result suggests that the remanent polarization might be $P_0 = 0{\cdot}065\,C\,m^{-2}$, surprisingly close to the values obtained experimentally, 0·05–$0{\cdot}06\,C\,m^{-2}$. In a sample in which the c axis is aligned parallel to the draw direction and the b axis is randomly oriented in the plane perpendicular to the c axis, the 60° model predicts that the maximum polarization would be reduced to $3P_0/\pi = 0{\cdot}062\,C\,m^{-2}$. For the rolled samples described in the previous paragraph, the maximum polarization would be $0{\cdot}056\,C\,m^{-2}$ if the initial orientation were perfect because the dipoles would all be oriented 30° from parallel to the normal to the film surface in the poled condition.

Broadhurst *et al.* [75] were the first to attempt to correct for a local field. They used an Onsager [76] cavity approach but the same result can be obtained more simply using the Lorentz field approximation [77]. The contributions to the electric field at the site of a dipole can be separated into three parts: the externally applied field, the Lorentz field, which is the field due to the polarization charge on the surface of a spherical cavity which is imagined to be created around the dipole with the dipole at the centre, and the field arising from the dipoles which were imagined to be removed to create the spherical cavity. It is well known that the Lorentz field is $P/3\kappa_0$, κ_0 being the permittivity of free space, and that the contribution from the sphere of dipoles is zero if the dipoles are aligned parallel and arranged on a cubic lattice.

To calculate the remanent polarization of PVF_2, Broadhurst *et al.* [75] assumed that the only non-zero contribution to the local field was the Lorentz field and that the polarizability of the dipoles was given by the Clausius–Mossotti relation

$$\alpha = \frac{3\kappa_0}{N}\frac{\kappa_\infty - 1}{\kappa_\infty + 2}, \tag{9}$$

where N is the density of dipoles and κ_∞ is the high-frequency, or electronic, dielectric constant. By adding the permanent and polarizable components of the dipole moments, the total polarization is found to be

$$P = \frac{\kappa_\infty + 2}{3} P_0, \tag{10}$$

with $P_0 = N\mu_0$ and $\mu_0 = 7 \times 10^{-30}$ C m. Mopsik and Broadhurst [78] and Kakutani [79] used $\kappa_\infty = 3$, and this model then predicts [17] that the remanent polarization of PVF_2 is 0·22 C m^{-2}, rather than 0·13 C m^{-2} as predicted by the rigid-dipole model. For a 50% crystalline material this model therefore predicts a remanent polarization of 0·11 C m^{-2}, significantly disagreeing with the experimental value of 0·05–0·06 C m^{-2}.

Purvis and Taylor [80, 81] calculated dipole field sums assuming point dipoles and found results which were quite different from the Lorentz field approximation. In fact this approximation led to the conclusion that the local field decreased the dipole moment of the dipoles and that the polarization of a PVF_2 crystal would be 0·086 C m^{-2}. Subsequently Al-Jishi and Taylor [82, 83] recalculated the local field taking into account the fact that the dipoles are extended rather than points. For dipoles consisting of $\pm 0{\cdot}43$ electronic charges separated by 0·10 nm, chosen by considering the size and dipole moment of the CF_2 unit, they found that the crystal remanent polarization would be 0·127 C m^{-2}, very close to the value of 0·131 C m^{-2}, obtained by assuming rigid dipoles and thus in good agreement with the experimental results.

Ogura and Chiba [84] have carried out calculations very similar to those of Taylor and co-workers and extended them to PVF_2 copolymers with F_3E. The results were essentially the same.

These calculations show that the polarization of the crystalline phase is very sensitive to the local field and to the structure of the lattice. It will therefore be very important to consider changes in the lattice when considering piezoelectric and pyroelectric coefficients as we shall discuss later.

2.3.3. *Kinetics of poling*

Early work on the poling process involved heating samples to some high temperature, typically above 80°C, applying a high electric field, 30 MV m^{-1} or higher,

and then cooling the sample to room temperature with the field applied. The effects of poling time, electric field and poling temperature were investigated by a number of groups [85–90]. It was found that the magnitude of the piezoelectric coefficient and of the induced polarization increases with increasing voltage and temperature, by about what might be expected within the electret hypothesis which tended to drive these studies.

Studies of the kinetics of the poling process have been far more fruitful. Buchman [91] studied polarization reversal switching currents at temperatures above 110°C and fields up to about 14 MV m^{-1}. He found that the switching current initially increased for a time after a reversal of the applied voltage, went through a maximum and then decreased to a low stable conductivity value. The current maximum J_{max} varied with electric field E and temperature T as

$$J_{max} = J_0 E^n \exp\left(-\frac{\alpha}{k_B T}\right), \tag{11}$$

with n varying from 0·7 to 1·6 and $\alpha = 0{\cdot}65$ eV. The reciprocal τ_{max}^{-1} of the time at which the current maximum occurred varied in a similar fashion:

$$\tau_{max}^{-1} = \tau_0^{-1} E^{n'} \exp\left(\frac{\beta}{k_B T}\right), \tag{12}$$

where $n' \geqslant n$ and β varied from 1·1 to 1·5 eV. At 140°C and a field of 14 MV m^{-1}, τ_{max} was about 30 s. The remanent polarization observed in these experiments was 0·08 C m^{-2}.

Blevin [90] studied the kinetics of the poling process by measuring the pyroelectric coefficient as a function of time during poling at a field of 100 MV m^{-1}. He reported poling times that ranged from 30 s for a poling temperature of 100°C to 5·5 days at a poling temperature of 20°C. The fact that poling could take place at room temperature

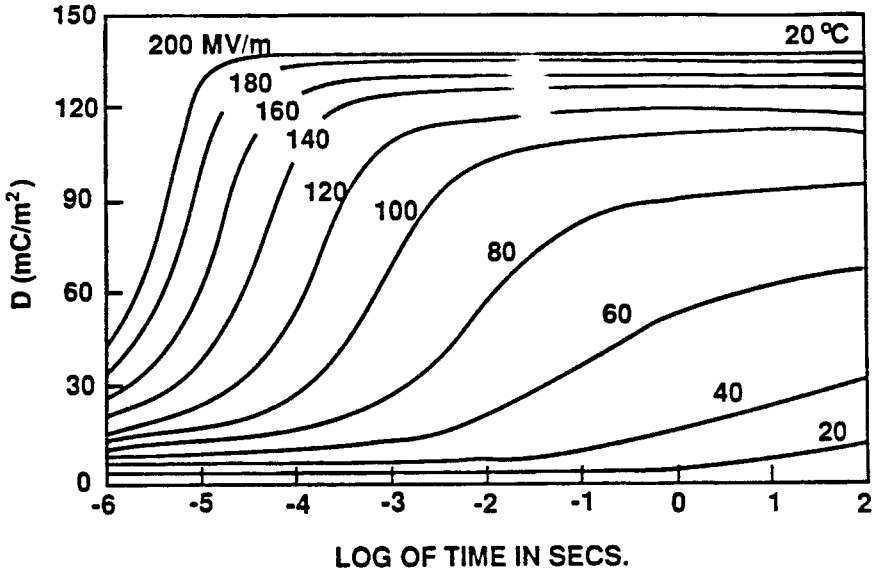

Figure 16. Time dependence of electric displacement at various electric fields and 20°C. (From Furukawa and Johnson [93].)

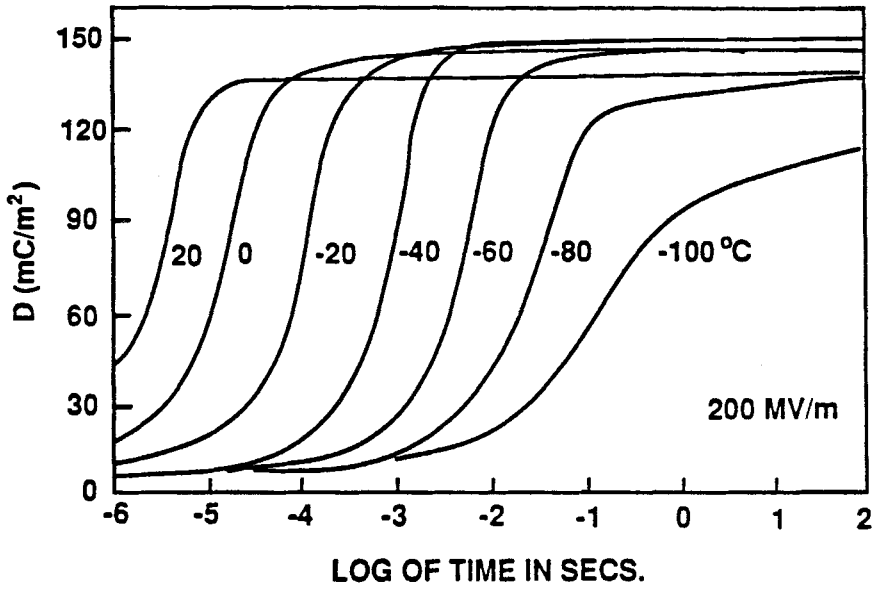

Figure 17. Time dependence of electric displacement at various temperatures and 200 MV m^{-1}. (From Furukawa and Johnson [93].)

and below was first reported by Southgate [61]. He used a corona to apply a very high field and reported that complete poling could be achieved in less than 1 s at room temperature. Hicks and Jones [92] also attempted to measure the poling time and found room temperature poling times of a few seconds for films 9 μm thick.

Furukawa and Johnson [93] were the first to apply very high fields and to measure the time dependence of the poling current at short times as a function of electric field and temperature. Their measurements were conducted up to fields of 200 MV m^{-1} and from −100 to 20°C. They observed a switching time of 4 μs at 20°C and 200 MV m^{-1} for films 7 μm thick. The time dependence of the electric displacement (integral of the poling current) observed at various electric fields and 20°C is shown in figure 16 and at various temperatures and 200 MV m^{-1} in figure 17.

Studies of ferroelectrics [10] have shown that in several materials the switching time follows either an exponential law

$$t_s \sim \exp\left(\frac{\alpha}{E}\right) \tag{13}$$

or a power law

$$t_s \sim E^{-n} \tag{14}$$

and phenomenological models have been developed, assuming nucleation-and-growth processes, which give these forms. When the experimental data were compared with these empirical relations [93, 94], the values of α and n for PVF_2 were found to be larger than those for better-known ferroelectrics, $\alpha = (1\text{–}2) \times 10^3$ MV m^{-1} and $n = 8\text{–}10$ for PVF_2 as against 1 MV m^{-1} and 1·5 for $BaTiO_3$ [10, 95–97]. The agreement between the experimental data and there two formulae was interpreted as evidence that the nucleation-and-growth process is dominant in PVF_2 also. Furukawa *et al.* [94] compared the shape of their switching currents with the predictions of a phenomenological theory developed by Wieder [98].

Clark and Taylor [99], on the other hand, have investigated the applicability of the kink or solitary wave propagation model [53] discussed above. In that model the time required for a kink to traverse a lamella was found to be negligible relative to the time for the creation of kinks and therefore the kink formation was the rate-limiting process. They assumed that this rate followed a decay rate form $\exp(-qt)$ with t the time and $q=q_0\exp[-(U-\lambda E)/k_BT]$, where q_0 is a constant and U is the zero-field energy barrier. They assumed that all barriers were identical and that the barrier height was reduced linearly by an applied field E with a constant of proportionality λ having the dimensions of a dipole moment.

It was assumed that the N polymer molecules in a crystalline region reoriented sequentially and then the time dependence of the polarization was calculated by summing over the distribution $Q(N)$ of N for all the crystallites:

$$P(t)=\sum_N Q(N)P_N(t). \tag{15}$$

In their calculation of the time dependence of the displacement $D(t)$ which could be compared with the experimental results of Furukawa and Johnson [93] they included the fact that the dielectric constant κ is time dependent:

$$D(t)=\kappa(t^{-1})\kappa_0E+P(t), \tag{16}$$

where $\kappa(t^{-1})$ is the real part of the dielectric function at frequency t^{-1} and κ_0 is the permittivity of free space. The frequency dependence of κ was taken from the measurements of Scheinbeim *et al.* [100] and extrapolated to higher and lower frequencies as necessary. For their calculations they used various distribution functions $Q(N)$ and found that all were in qualitative agreement with the experimental results of Furukawa and Johnson. An example of the agreement obtained, with

$$Q(N)\sim N\exp(-N/N_0),$$

is shown in figure 18 where the displacement is plotted against the logarithm of time.

Clark and Taylor [99] pointed out that their model implies that $\log t_s$ varies linearly with E whereas Furukawa and Johnson suggested that $\log t_s$ varies linearly as $1/E$. They argued that the two models agreed equally well with the experimental data between 120 and 200 MV m^{-1} but that at lower fields, down to 80 MV m^{-1}, both formulae break down; however, the model of Furukawa and Johnson breaks down more slowly. The logarithm of the switching time data of Furukawa and Johnson [93] are plotted against $1/E$ in figure 19 (*a*) and against E in figure 19 (*b*).

Odajima *et al.* [101] have investigated the nucleation-and-growth model in more detail, attempting to combine it with aspects of the kink propagation model [53]. Al-Jishi and Taylor [102], however, have calculated the local electric field and concluded that it is sufficiently strong to pose difficulties for any interpretation of switching in terms of a macroscopic model of nucleation and growth. Takase and Odajima [103] and Takase *et al.* [104] have investigated the effect of large doses of radiation on the switching process and suggested that two nucleation processes were involved.

Polarization reversal in PVF_2 copolymers has also been investigated by Furukawa *et al.* [105, 106]. For films 20 μm thick 65 mol% VDF–35 mol% F_3E copolymer they found [105] very rapid switching transients which could be fit with the function $1-\exp[-(t/t_s)^n]$, where n could be as large as 5. They also found a remanent polarization of 0·08 C m^{-2}. Spin-coated thin films of 52 mol% VDF–48 mol% F_3E, 65 mol% VDF–35 mol% F_3E and 73 mol% VDF–27 mol% F_3E copolymers were also

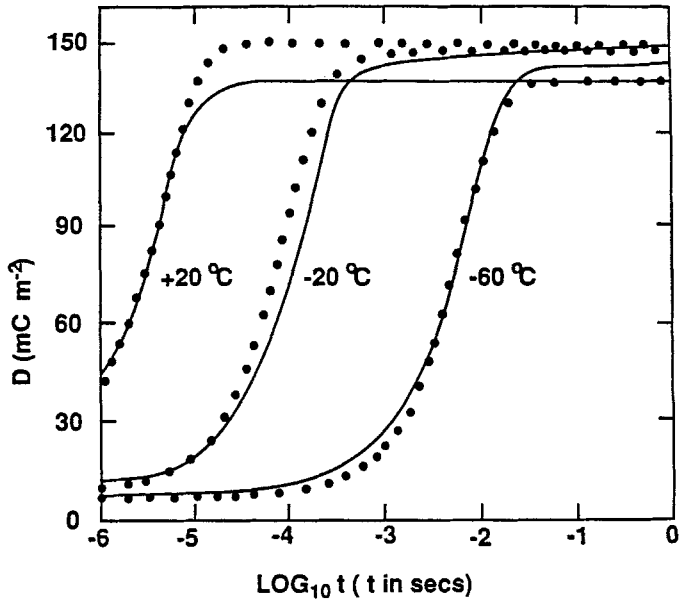

Figure 18. A comparison of the theory of Clark and Taylor (●) with some of the experimental data of Furukawa and Johnson (——). (From Clark and Taylor [99].)

investigated [106]. Switching times as short as 100 ns were observed and the switching times for the three copolymers were the same. Film thickness apparently is not a factor. They reported no variation over the range 0·3–1·5 μm and a film of the 73 mol% VDF–27 mol% F_3E copolymer which was 15 μm thick was found to have the same switching time as the thinner films, at least at the lower fields. Since so much has been made of the field dependence, it is worth pointing out that the 52 mol% VDF–48 mol% F_3E film did not follow the simple exponential law $t_s \sim \exp(\alpha/E)$ as the other two copolymers did. The discrepancy was attributed to this copolymer's disordered crystal structure in the ferroelectric phase [107, 108]. Polarization switching and other ferroelectric properties in thin (0·06–2·5 μm) films of a 75 mol% VDF–25 mol% F_3E copolymer have been investigated by Kimura and Ohigashi [109, 110].

The polarization switching process is very complicated and it is not clearly understood in any ferroelectric. Very large electric fields are involved. If two adjacent crystals of PVF_2 were stacked one on top of the other with their polarizations parallel and vertical and then the polarization of one crystal suddenly reversed, the difference in electric field between the two crystals would be of the order of 10^4 MV m^{-1}, clearly greater than the high-voltage breakdown field strength. It is clear that the high fields developed during the polarization process have to be taken into account, but how to accomplish that is far from clear. Many studies have been devoted to studies of domains in more familiar ferroelectrics [10] but none has been reported for PVF_2. Spiking can be observed in the poling current [111] which is reminiscent of Barkhausen pulses [10] but detailed investigations have not been undertaken.

In summary, the polarization switching process in PVF_2 is in many ways similar to that in more conventional ferroelectrics except that the coercive field is considerably higher and a kink propagation process such as that envisaged by Dvey-Aharon *et al.* [53] is almost certainly involved.

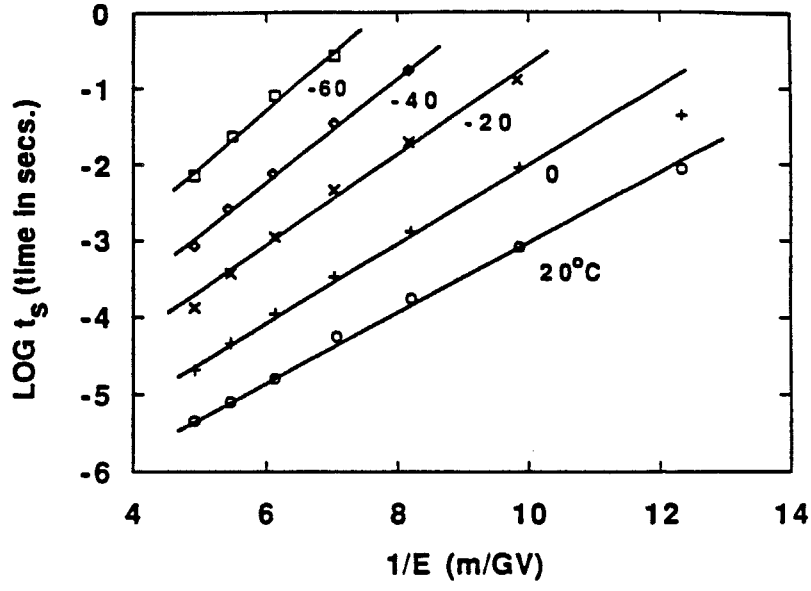

(*a*)

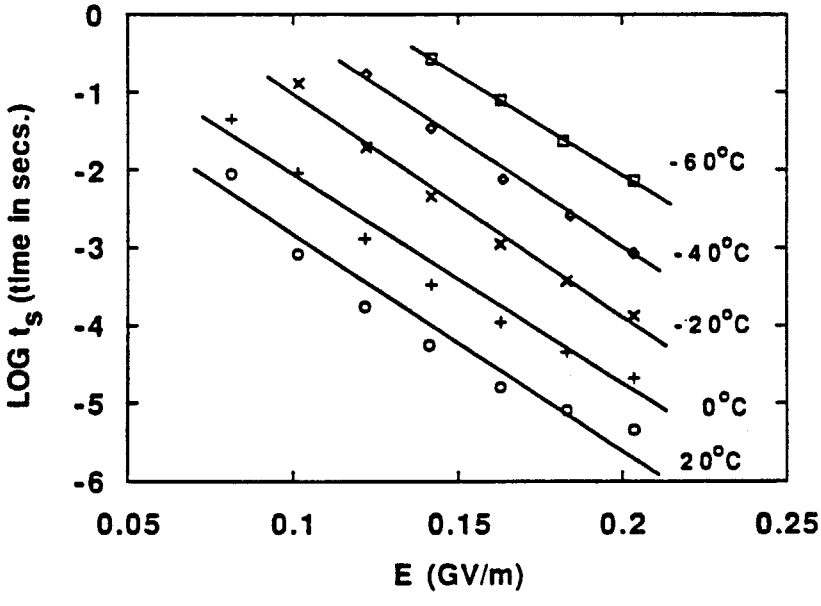

(*b*)

Figure 19. The logarithm of the switching time t_s in PVF_2 plotted against (*a*) the reciprocal of the applied field E and (*b*) the applied field E. (Data from Furukawa and Johnson [93].)

2.3.4. *Ferroelectric phase transition*

The PVF_2 β-phase melts in the approximate range 175–180°C [13] and no evidence of a ferroelectric transition is seen prior to melting. In copolymers with F_3E or F_4E and in heavily defected (HHTT defects) PVF_2, the ferroelectric-to-paraelectric phase transition is observed, and in this section we shall describe some of the results of these studies.

In 1979–1981 Yagi and coworkers synthesized a complete range of compositions of copolymers of VDF and F_3E [112, 113] and undertook a variety of studies of their properties [114–116], including infrared, X-ray and dielectric constant measurements. Of perhaps most interest, differential scanning calorimetry (DSC) scans showed endothermic peaks well below the melting peaks, at temperatures which depended strongly on the copolymer composition. The data are shown in figure 20. They also observed anomalies in the dielectric constant coincident in temperature with the low-temperature peak in the DSC scans. Kitayama *et al.* [117] and Yamada *et al.* [118] concentrated on 51 mol% VDF–49 mol% F_3E copolymers and reported that there was a peak in the DSC scan near 65°C. They also reported that the piezoelectric and pyroelectric coefficients vanished above 70°C, that the dielectric constant peaked near 70°C and that there was a large increase in the thermal expansion coefficient between 40 and 80°C. Using X-ray diffraction they also found a large increase in the volume of the unit cell between room temperature and 85°C. They concluded that the transition near 65°C was a ferroelectric-to-paraelectric phase transition that it was of first order. The observation of the endothermic peak was cited as the primary evidence for a first-order transition.

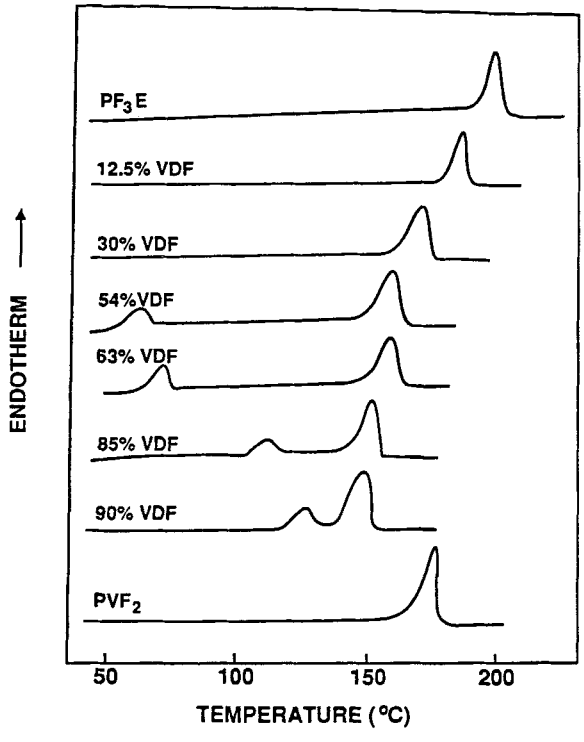

Figure 20. DSC scans of VDF–F_3E copolymers of different mole percentage ratios and of the PVF_2 and poly(trifluorethylene) (PF_3E) homopolymers. (From Yagi *et al.* [115].)

A number of other groups reported similar observations for compositions near 50 mol% at about the same time [119–124].

Lovinger *et al.* [107] undertook a careful X-ray diffraction study of 52 mol% VDF–48 mol% F_3E copolymer and found that melt-solidified samples consist of a mixture of two disordered crystalline phases, one *trans* planar, the other 3/1 helical. Either the application of an electric field or stretching transforms the disordered mixture of phases into a well ordered planar zigzag phase. Heating to a high temperature results in the formation of the disordered 3/1 helical structure analogous to that of poly(trifluoroethylene) [125] and the original disordered mixture of phases is recovered upon cooling to room temperature.

The crystal structure and its dependence on temperature and monomer mole ratio for the VDF–F_3E copolymers has undergone intense scrutiny [108, 126–130] but agreement remains incomplete [131] regarding the crystal structure change occurring at the Curie temperature.

It has now been found that VDF–F_4E copolymers with 72–82 mol% VDF [132–135] and that PVF_2 which has been specially synthesized to contain 13·1–15·5 mol% HHTT defects [135] also exhibit ferroelectric-to-paraelectric phase transitions. The transitions are complicated, occur over fairly wide temperature ranges and exhibit a coexistence of the ferroelectric and paraelectric phases, hysteresis, latent heat and a discontinuous change in the interplanar spacing. They are clearly first order.

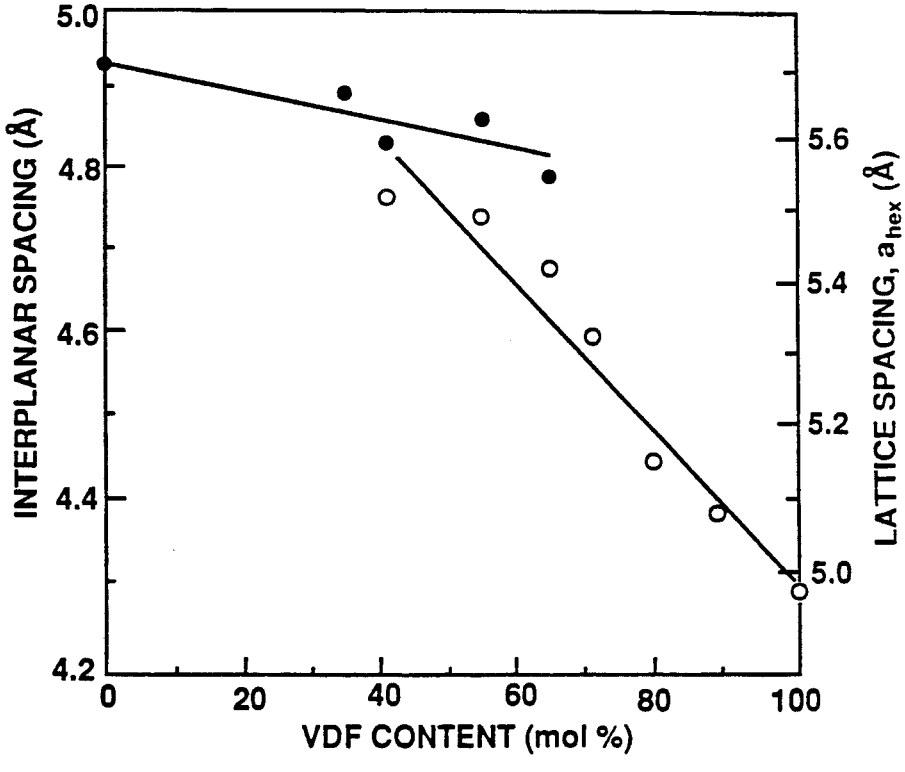

Figure 21. Interplanar and lattice spacing plotted against VDF concentration in VDF–F_4E copolymers: (●), data for the polytetrafluoroethylene-like disordered non-polar phase; (○), β-phase. (From Lovinger *et al.* [135].)

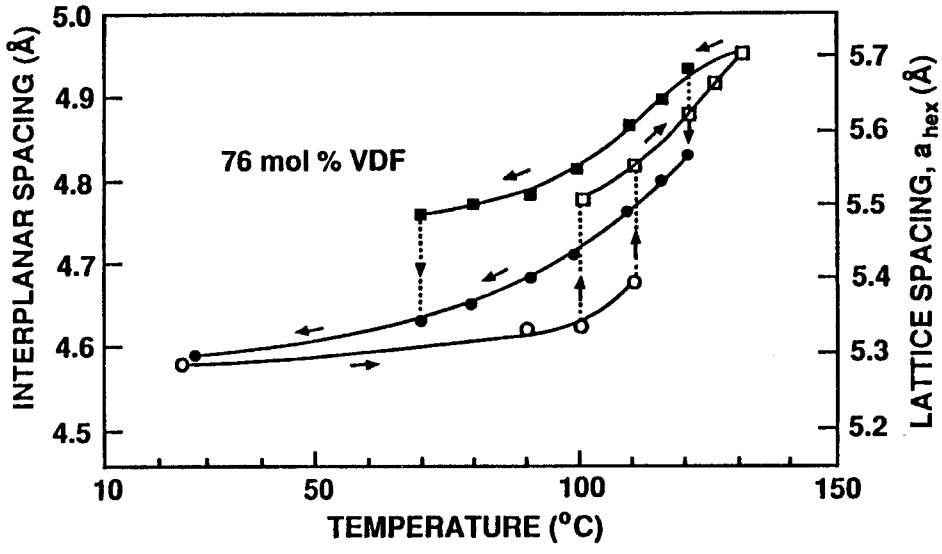

Figure 22. Interplanar spacings observed in a 76 mol% VDF–24 mol% F_4E copolymer as a function of temperature: (○) spacings observed for the ferroelectric phase, heating cycle; (●), spacings observed for the ferroelectric phase, cooling cycle; (□), spacings observed for the paraelectric phase, heating cycle; (■), spacings observed for the paraelectric phase, cooling cycle. (From Lovinger *et al.* [135].)

It appears that in all these materials that as defects, HHTT or monomer units with extra fluorine atoms, F_3E or F_4E are added, the distance between the molecules increases. The interplanar and lattice spacing as a function of VDF concentration obtained by Lovinger *et al.* [135] for VDF–F_4E copolymers is shown in figure 21. The additional space lowers the energy required to form *gauche* and *gauche'* bonds. At lower defect concentrations the most stable conformation at room temperature is the α-phase. As the defect concentration is increased the β-phase which is ferroelectric becomes the most stable, as predicted by Farmer *et al.* [22]. Curie transitions are observed in the β-phase material unless melting intervenes. At even higher defect concentrations the disordered paraelectric phase is the stable phase at ambient temperature and ferroelectricity is not observed. Also, as the defect concentration increases from low concentrations, the intramolecular order decreases but the intermolecular order tends to increase. At ambient temperature the materials which exhibit a ferroelectric phase transition frequently exist in both the paraelectric and the ferroelectric phases in different crystalline regions and the application of a high electric field or stretching quickly converts it to the ferroelectric phase. As the temperature is increased, the transformation from the ferroelectric to the paraelectric phase is seen to occur over some temperature range, and the amount of one phase decreases gradually while the concentration of the other phase increases. When the temperature is lowered from the paraelectric phase, the reverse happens, at a lower temperature and over a larger temperature range. The interplanar and lattice spacings observed [135] as a function of temperature for a 76 mol% VDF–24 mol% F_4E copolymer are shown in figure 22.

It is quite clear that ferroelectric phase transitions occur in defected PVF_2 and that the temperature at which the transition occurs depends on the concentration and type

of defect. Lovinger has used this fact to estimate the Curie temperature for the PVF_2 homopolymer. He plotted the Curie temperature against VDF concentration for VDF–F_4E copolymers and extrapolated to pure VDF. The graph is shown in figure 23. This procedure led to an estimate for the Curie temperature for PVF_2 of 195°C, well above the melting temperature of 175°C as expected.

2.3.5. *Summary*

In this section we have attempted to present the evidence that PVF_2 is indeed ferroelectric and to discuss some of the ferroelectric properties. The crystal structure is polar and both X-ray diffraction and infrared spectroscopic studies have shown that the application of a high electric field can change the direction of polarization of the crystalline regions. Theoretical models have been developed which are in reasonable agreement with the experimental results, including the kinetics of the poling process. The remanent polarization is near $0{\cdot}060\,C\,m^{-2}$ and the coercive field is high, of the order of $80\,MV\,m^{-1}$. The Curie temperature is not observable in PVF_2 because it is above the melting temperature but ferroelectric-to-paraelectric transitions can be observed in highly defected PVF_2, where the defects are produced by the addition of F_3E, F_4E or HHTT units.

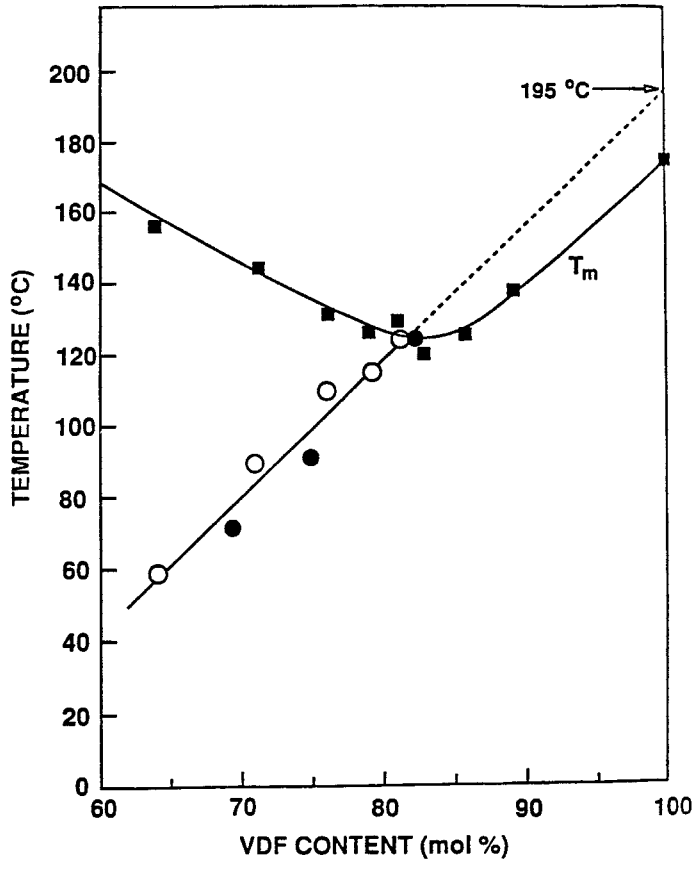

Figure 23. Curie temperature (○, ●) and melting temperatures (■) plotted against VDF content for VDF–F_4E copolymers. (From Lovinger *et al.* [134].)

2.4. *Pyroelectricity and piezoelectricity*

2.4.1. *Definitions*

The pyroelectric coefficient p and piezoelectric coefficient are defined as the change in polarization P resulting from a change in temperature T or an applied stress σ respectively:

$$\Delta P = p\,\Delta T \tag{17}$$

and

$$\Delta P = d\sigma. \tag{18}$$

Piezoelectric and pyroelectric materials are anisotropic, however, and to describe the polarization adequately P must be a vector with three orthogonal components in the 1, 2 and 3 directions and

$$\Delta P_i = p_i \Delta T, \tag{19}$$

where i takes the values 1, 2 or 3. In polymers the common practice is to label the three orthogonal directions as follows: 1 is parallel to the draw direction which tends to be parallel to the chain axis, 2 is in the plane of the film and perpendicular to the draw direction and 3 is perpendicular to the film surface. For the pyroelectric coefficient, only α_3 has been measured.

The stress within a solid is specified by a second-rank tensor σ_{ij}, where i and j equal 1, 2 or 3. The meaning of a component σ_{ij} is easily understood if the coordinate system is assumed to be centred in a volume element in the form of a cube which has edges of unit length parallel to the coordinate axes. The ith component of the force exerted on the face of the cube is specified by the subscript i, while the subscript j indicates that the force is applied to the face of the cube perpendicularly intersecting the $+j$ axis. According to this definition, tensile stresses result in positive value of σ_{11}, σ_{22} and σ_{33}. Components for which $i \neq j$ are called the shear components. One may readily observe that in the absence of body torques, which is the usual case, $\sigma_{ij} = \sigma_{ji}$.

Symmetry of the stress tensor about the diagonal allows a more compact description of the state of stress, the matrix notation. The two subscripts may be simplified to a single one, which equals 1–6. In this notation, subscripts 4, 5 and 6 represent the shear stresses 23, 31 and 12 respectively. A comprehensive treatment of tensor and matrix notation has been given by Nye [12].

The direct piezoelectric effect, as opposed to the converse effect which will be defined later, is a linear relationship between the polarization and the applied stress when the electric field and temperature are held constant. Each of the three components of the polarization, in general, is related to each of the nine stress components, and the coefficients d form a third-rank tensor having 27 components. Thus

$$\Delta P_i = d_{ijk}\sigma_{jk}, \tag{20}$$

where repeated subscripts imply summation. The d_{ijk} are called the piezoelectric strain coefficients.

A more compact notation is possible, as described above, because of the symmetry of σ_{ij}. When the terms of equation (20) are written out, terms arising from shear stress may be written in pairs such as

$$d_{312}\sigma_{12} + d_{321}\sigma_{21} = (d_{312} + d_{321})\sigma_{12} \tag{21}$$

in the absence of body torques. If d_{ijk} is set equal to d_{ikj}, the matrix notation may be employed to combine the last two subscripts of d_{ijk} into a single subscript, so that

$$\Delta P_i = d_{im}\sigma_m, \tag{22}$$

where $m = 1$–6. The components of d_{im} are equal in value to the corresponding d_{ijk} if m is 1, 2 or 3; otherwise, d_{im} is twice the corresponding tensor component.

The 18 coefficients d_{im} provide a complete description of the linear relationship between polarization and stress, although crystal symmetries often reduce the number of independent coefficients.

The piezoelectric coefficient described above is the direct piezoelectric coefficient as pointed out previously. The application of an electric field produces a strain and the piezoelectric coefficients which describe the linear relationship between the electric field and the strain are referred to as the converse piezoelectric coefficients. Usually it is stated that the direct and converse coefficients are equal but, as we shall discuss later, we have shown that they are not and that in polymers the difference can be very large [136].

The strain within a solid can be specified from the change in a vector $\boldsymbol{x}$ connecting two points when the solid is deformed. The tensor quantities δ_{ij} are defined as the dimensionless ratios of components of Δx (the change in the vector $\boldsymbol{x}$) to the components of $\boldsymbol{x}$:

$$\delta_{ij} = \lim_{x \to 0} \left(\frac{\Delta x_i}{x_j} \right). \tag{23}$$

When the subscripts are equal, the quantities δ_{ij} measure the increase in length per unit length parallel to the i axis. Otherwise, δ_{ij} is equal, for strains small compared with unity, to the angular rotation towards the i axis of a line parallel to the j axis before the deformation.

It is clear from the above that, if $\delta_{ij} = -\delta_{ji}$, the solid has undergone a rigid rotation without deformation. The tensor shear strains δ_{ij} are therefore defined as the symmetrical part of δ_{ij}, so that they are insensitive to rigid rotations:

$$\varepsilon_{ij} = \tfrac{1}{2}(\delta_{ij} + \delta_{ji}). \tag{24}$$

The tensile strains ε_{ii} are unaffected by this transformation.

To convert the strains to matrix notation, ε_m is defined as ε_{ii} when $m = 1$, 2 or 3, but ε_m is twice the corresponding tensor component when $m = 4$, 5 or 6.

Strains are related to stresses through the fourth-rank elastic compliance tensor:

$$\varepsilon_{ij} = s_{ijkl}\sigma_{kl}. \tag{25}$$

The inverse relation is

$$\sigma_{ij} = c_{ijkl}\varepsilon_{kl}, \tag{26}$$

where c is the elastic stiffness. The 81 components of either s or c may be reduced to 36 by means of the matrix notation in which the first and last pairs of subscripts are each collapsed into a single subscript which equals 1–6:

$$\varepsilon_m = s_{mn}\sigma_n, \tag{27}$$

$$\sigma_m = c_{mn}\varepsilon_n. \tag{28}$$

The s_{mn} components are equal to the corresponding tensor components multiplied by the factor 1, 2 or 4, depending on whether neither, either or both m and n are greater than 3 respectively. No multiplying factors are needed with the components c_{mn}.

We are now in a position to define the converse piezoelectric coefficients d^c_{ijk} which express the linear relationship between the strain and the applied electric field E at constant stress and temperature:

$$\varepsilon_{jk} = d^c_{ijk} E_i. \tag{29}$$

In matrix notation this equation is

$$\varepsilon_m = d^c_{im} E_i, \tag{30}$$

where $m = 1$–6. Generally it is believed that the converse piezoelectric coefficient is equal to the direct coefficient [10, 12, 137], as we mentioned above, but we are distinguishing between them because later in this review we shall show that they are different.

It is important to point out that care must be taken in comparing the measured piezoelectric and pyroelectric coefficients with the coefficients defined above. An experimental measurement consists typically in applying a stress or changing the temperature and measuring the charge exchanged between the shorted electrodes. The electrodes typically consist of very thin evaporated metal films which deform with the sample and thus the measured charge in the experiment when a stress is applied is

$$\frac{\partial Q}{\partial \sigma} = A \frac{\partial P}{\partial \sigma} + P \frac{\partial A}{\partial \sigma}, \tag{31}$$

where Q is the measured charge and A is the area of the electrodes. The change in polarization is then

$$\frac{\partial P}{\partial \sigma} = \frac{1}{A} \frac{\partial Q}{\partial \sigma} - \frac{P}{A} \frac{\partial A}{\partial \sigma}. \tag{32}$$

The necessity of correcting the experimental data with the second term on the right-hand side of equation (32) has long been recognized but the correction is usually small. In pliable polymers, however, it can become dominant. Dvey-Aharon and Taylor [138] have discussed this correction in some detail.

2.4.2. *Pyroelectricity*

2.4.2.1. *Magnitude and temperature dependence.* Pyroelectricity is a linear reversible change in polarization brought about by a change in temperature when the electric field is held constant. The pyroelectric coefficients p_i are defined by

$$\Delta P_i = p_i \Delta T. \tag{33}$$

In polymers the pyroelectric coefficient is usually measured by shorting the electrodes on opposite sides of a thin film together and measuring the amount of charge exchanged between the two electrodes when the sample temperature is changed a known amount. It is possible to measure the voltage developed across a capacitor connected between the two electrodes to measure the amount of charge, but this procedure introduces some error because the electric field between the two electrodes affects the magnitude of the change in polarization.

Pyroelectricity in PVF_2 was first reported by Bergman and co-workers [6–8]. They reported values of about $-2{\cdot}4 \times 10^{-5}\,C\,m^{-2}\,K^{-1}$ for biaxially oriented films (films stretched in two perpendicular directions in the plane of the film during manufacture) and about $0{\cdot}5 \times 10^{-5}\,C\,m^{-2}\,K^{-1}$ for uniaxially oriented films.

Initially there were question raised about how reversible pyroelectricity was in PVF_2 [85, 139] because it was found that the magnitude of the coefficient depended on how high the sample had been heated after poling. We now know that the magnitude of the remanent polarization is reduced when a sample is annealed at elevated temperatures [45] and that the value reported by Pfister *et al.* [85] (-4×10^{-6} C cm^{-2} K^{-1}) was low because they had annealed their sample at 120°C after poling. Bur *et al.* [45] in fact showed that the pyroelectric coefficient is proportional to the remanent polarization.

The magnitude of the pyroelectric coefficient reported by different groups differs, presumably because of different sample preparation techniques, but it tends to be near that reported by Bergman *et al.* [6]. For example, Kepler and Anderson [140] reported $-1{\cdot}25 \times 10^{-5}$ and $-2{\cdot}74 \times 10^{-5}$ C m^{-2} K^{-1} for biaxially and uniaxially oriented samples respectively.

There seems to be little agreement on the temperature dependence, however. Burkard and Pfister [139] reported a monotonically increasing magnitude from about $-1{\cdot}5 \times 10^{-6}$ C m^{-2} K^{-1} at −100°C to -8×10^{-6} or -9×10^{-6} C m^{-2} K^{-1} at 75°C for samples which had been poled at 112°C in a field of 30 MV m^{-1} and then annealed at 112°C. They heated and cooled their sample at a constant rate and measured the current between the electrodes. Some of their experimental data are shown in figure 24. Buchman [91] and Tamura *et al.* [48] used a pulsed-heating technique. Periodic heat pulses were applied to samples by chopping a light beam while the temperature was varied and the a.c. signal was measured. Buchman found that the pyroelectric coefficient at −180°C was about equal to that at 100°C and that it went through a minimum near the glass transition temperature at about −50°C. The minimum was about one fifth of the maximum. The magnitude of the coefficient was not determined.

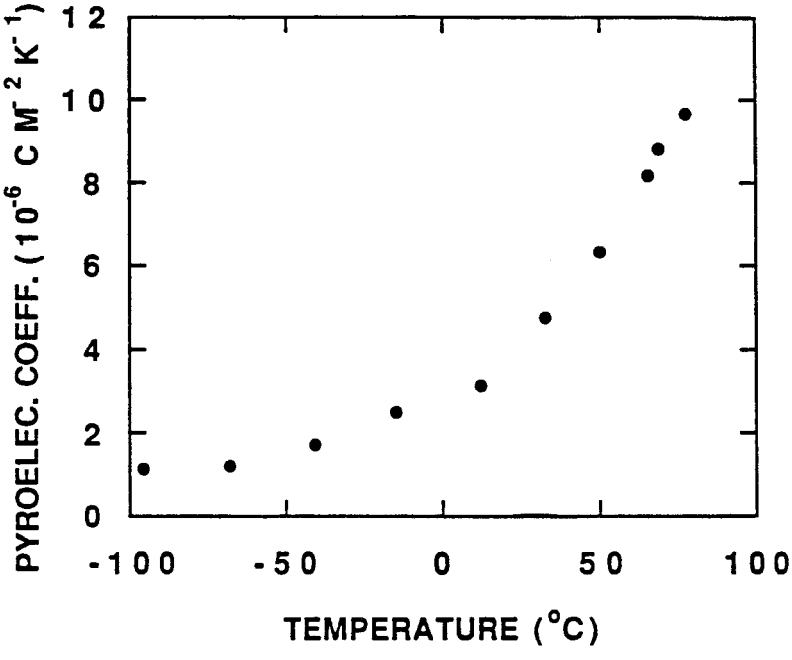

Figure 24. Pyroelectric coefficient plotted against temperature. (Data from Burkard and Pfister [139].)

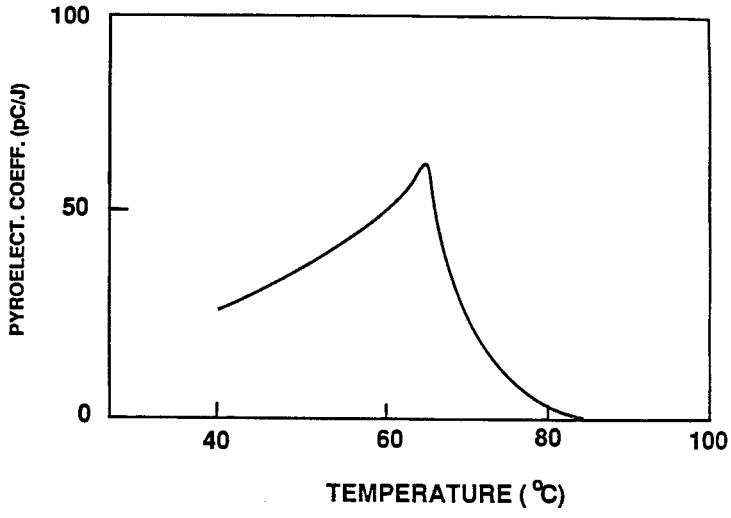

Figure 25. Pyroelectric coefficient plotted against temperature for 52 mol% VDF–48 mol% F_3E copolymer. (Redrawn from Date [141].)

Tamura *et al.* reported that the pyroelectric coefficient is approximately constant from −80 to 50°C. Date [141] has measured the temperature dependence of the pyroelectric coefficient in a 52 mol% VDF–48 mol% F_3E copolymer using a chopped light beam and lock-in a.c detection. His results are shown in figure 25.

2.4.2.2. *Primary and secondary pyroelectricity.* Pyroelectricity can be separated into two parts, namely primary and secondary, and, in order to determine the contributions from different possible mechanisms, it is useful to measure the two parts experimentally. Primary pyroelectricity is that part which is observed when the sample dimensions are clamped while the temperature is changed. Secondary pyroelectricity is the additional contribution to the polarization observed when the sample is subsequently allowed to relax to its equilibrium dimensions, and it often accounts for the majority of the pyroelectric response. Secondary pyroelectricity should not be confused with the contribution to an experimental signal which arises from a change in sample and thus electrode dimensions, as some workers have done. It is defined as the change in polarization, and not the change in charge on the electrodes, which results from changes in the sample dimensions [10].

Secondary pyroelectricity results from piezoelectricity and the relationship between the secondary pyroelectric coefficients p_i^s can be derived by combining equations (28) and (22) with the definition of the thermal expansion coefficients which in matrix notation is

$$\varepsilon_i = \alpha_i \Delta T. \tag{34}$$

The result is

$$p_i^s = d_{im} c_{mn} \alpha_n. \tag{35}$$

The experimentally measured pyroelectric coefficients, such as the direct piezoelectric coefficients, need correction if the change in polarization in equation (33) is

required. The correction terms have the form $(P/A)(\partial A/\partial T)$ and are the products of the polarization and thermal expansion coefficients. These terms can be comparable in size with the measured pyroelectric coefficients of polymers. Interestingly enough, either the experimental or the corrected p and d coefficients may be used in equation (35), provided that they are used consistently. The effects of the correction are the same on both sides of the equation.

In a recent review [142], it was concluded that the pyroelectric effect in ferroelectric polymers is dominated by what was called the primary effect. The primary effect was defined in the standard way as the intrinsic pyrolectricity occurring in a clamped sample while the secondary effect arises from the coupling between piezoelectricity and thermal expansion. The secondary contribution was approximated by calculating the change in polarization resulting from changes in sample thickness with temperature in a rigid-dipole model. All other possible contributions were ignored and, since the calculated value was small relative to the experimentally observed value, the conclusion was made that primary pyroelectricity dominated.

Kepler and Anderson [140, 143] have conducted a series of experiments to determine the relative contributions of primary and secondary pyroelectricity in PVF_2 and thus to gain insight into the fundamental mechanisms involved. The piezoelectric, thermal expansion and elastic coefficients of uniaxially and biaxially oriented PVF_2 films were measured and used to calculate the secondary pyroelectric coefficient from equation (35) and the results were compared with the experimentally measured pyroelectric coefficient [140]. The quantities determined in these experiments are shown in table 1. Secondary pyroelectricity accounted for approximately half the pyroelectricity observed.

Table 1. Piezoelectric, pyroelectric and thermal expansion coefficients and mechanical properties of PVF_2 thin films. (From Kepler and Anderson) [140].)

		Biaxially oriented film	Uniaxially oriented film
Piezoelectric coefficients ($pC\,N^{-1}$)	d_{31}	4·34	21·4
	d_{32}	4·36	2·3
	d_{33}	−12·4	−31·5
	d_h	−4·8	−9·6
	d_{33}[a]	−13·5	−33·3
Pyroelectric coefficients ($10^{-5}\,C\,m^{-2}\,K^{-1}$)	p_3	−1·25	−2·74
	p_3^s (calculated)	−0·44	−1·48
Thermal expansion coefficients ($10^{-4}\,K^{-1}$)	α_1	1·24	0·13
	α_2	1·00	1·45
Mechanical properties	E (10^9 Pa)	2·5	2·5
	K ($10^{-10}\,Pa^{-1}$)	2·6	2·6
	ν	0·392	0·392
	s_{11} ($10^{-10}\,Pa^{-1}$)	4·0	4·0
	s_{12} ($10^{-10}\,Pa^{-1}$)	−1·57	−1·57
	c_{11} (10^9 Pa)	5·04	5·04
	c_{12} (10^9 Pa)	3·25	3·25

[a] Calculated from the hydrostatic piezoelectric coefficients d_{31} and d_{32}.

An experiment was then undertaken to observe the primary pyroelectricity. Lightly dyed samples were heated suddenly with 200 ps laser light pulses and the time dependence of the appearance of the pyroelectric charge measured [143]. Since inertial effects would clamp the sample dimensions, it was anticipated that charge from primary pyroelectricity would appear as rapidly as the sample was heated and that the charge from secondary pyroelectricity would appear as the sample dimensions relaxed to the new equilibrium dimensions. No evidence for a significant primary contribution was observed and subsequent experiments [144] led to the conclusion that the primary pyroelectricity contribution to the total pyroelectric effect can be no larger than 15%. The magnitude of the pyroelectric effect observed in the pulsed-heating experiments (the pyroelectric signal was observed for times up to about 1 μs) was again about half the total pyroelectric effect observed in experiments [140] in which the sample was heated by transferring it from one oil bath to another with an accurately known temperature difference. These results indicated that another slow process was contributing significantly and the suggestion was made that reversible changes in crystallinity were occurring [143]. Kavesh and Schultz [145] in a study of polyethylene had concluded that its crystallinity decreases reversibly from 67% at 25°C to 57% at 110°C and that the magnitude of a change in crystallinity in PVF_2 alone would result in a pyroelectric coefficient of $-5{\cdot}9 \times 10^{-5}\,C\,m^{-2}\,K$, more than twice the experimentally observed value.

Nix *et al.* [146] have conducted a series of experiments which led them to conclude that, depending on the method of manufacture, the primary contribution to the total pyroelectric coefficient in PVF_2 varied from 90% to 40%. However, they calculated the secondary pyroelectricity contribution from equation (35) and assumed that the remainder is primary pyroelectricity. It seems highly likely that most, if not all, the remainder results not from primary pyroelectricity but from reversible changes in crystallinity with temperature, as will be discussed in the next section. We consider these changes in crystallinity to be outside the scope of the standard definition of primary and secondary pyroelectricity because they involve changes in the state of the sample.

2.4.2.3. *Reversible changes in crystallinity.* A number of experiments have now been conducted which confirm that indeed reversible crystallinity is contributing to the pyroelectric coefficient in PVF_2. Schultz *et al.* [147] made temperature-dependent small-angle X-ray scattering measurements and the results were interpreted as evidence for reversible crystallinity. Anderson *et al.* [148] measured the time dependence of the appearance of pyroelectric charge after a sudden change in temperature which resulted from absorption of a 200 ps laser light pulse. A gradual increase in charge, which occurs between about 1 μs and 1 s and accounts for 25% of the total pyroelectric charge, was attributed to reversible changes in crystallinity.

Kepler and co-workers [144, 149, 150] pointed out that, if indeed the crystallinity changes reversibly with temperature, thermodynamic relations indicate that it should also change with an applied electric field. Since the Gibbs free energy G given by

$$G = u + pv - sT - PE \tag{36}$$

does not change crossing a phase boundary, changes in G along the boundary are equal in the two phases. In this equation, p is the pressure, T is the temperature, v and s are the molar volume and entropy respectively and P is the component of the molar electric

moment parallel to the electric field E. If we consider the amorphous–crystalline phase boundary, then $dG_a = dG_c$ and, since [151]

$$du = T\,ds - p\,dv + E\,dP,$$

then

$$dG = v\,dp - s\,dT - P\,dE$$

and, since p is constant

$$s_c\,dT + P_c\,dE = s_a\,dT + P_a\,dE, \tag{37}$$

where the subscripts a and c denote the amorphous and crystalline phases respectively. Therefore

$$(s_c - s_a)\,dT = (P_c - P_a)\,dE \tag{38}$$

and, since $(s_c - s_a)T = l$, where l is the molar latent heat of melting, the change dT_m in the melting temperature resulting from a change dE in the applied electric field is

$$dT_m = \frac{TP_c\,dE}{l} \tag{39}$$

under the simplifying assumption that $P_a = 0$.

In order to calculate the magnitude of the change in crystallinity caused by an electric field, it is assumed that some fraction γ of the pyroelectric coefficient p results from reversible changes $d\chi_c/dT$ in crystallinity with temperature. Therefore, with the approximation of perfect alignment of the crystallites,

$$\frac{d\chi_c}{dT} = \frac{\gamma p}{P_c}. \tag{40}$$

To calculate the change in crystallinity produced by the application of an electric field, equations (39) and (40) are combined to produce

$$\frac{d\chi_c}{dE} = -\frac{d\chi_c}{dT}\frac{dT_m}{dE} = -\frac{\gamma pT}{l}. \tag{41}$$

Equation (41) relies on the assumption that a field-induced change in the melting temperature results in the same amount of melting or crystallization at constant temperature as an actual change in temperature of the same amount but of the opposite sign.

Therefore, to test the hypothesis that reversible changes in crystallinity were contributing significantly to the pyroelectric coefficient, Kepler and co-workers [144, 149, 150] undertook experiments to measure the change in intensity of X-rays diffracted from the 200 and 110 planes in PVF_2 as a function of an applied field. The experimental results are shown in figure 26. The latent heat of melting of the crystalline phase at 298 K was estimated to be 55 J g^{-1}, on the basis of measurements of the heat of melting, an estimated crystallinity of 0·5 and measurements of the heat capacities of the amorphous and crystalline phases. The molar latent heat l is $3{\cdot}52 \times 10^3$ J mol^{-1} using the molecular weight of the monomer or repeat unit, 64 g, as the molar unit. The molar pyroelectric coefficient was determined to be $-9{\cdot}8 \times 10^{-10}$ C m K^{-1} mol^{-1} by using the average density [13] for PVF_2 of 1·76 g cm^{-3} and $-2{\cdot}7 \times 10^5$ C m^{-2} K^{-1} from table 1 for the volume pyroelectric coefficient. With these values and the assumption that one third of the pyroelectric coefficient results from reversible changes in

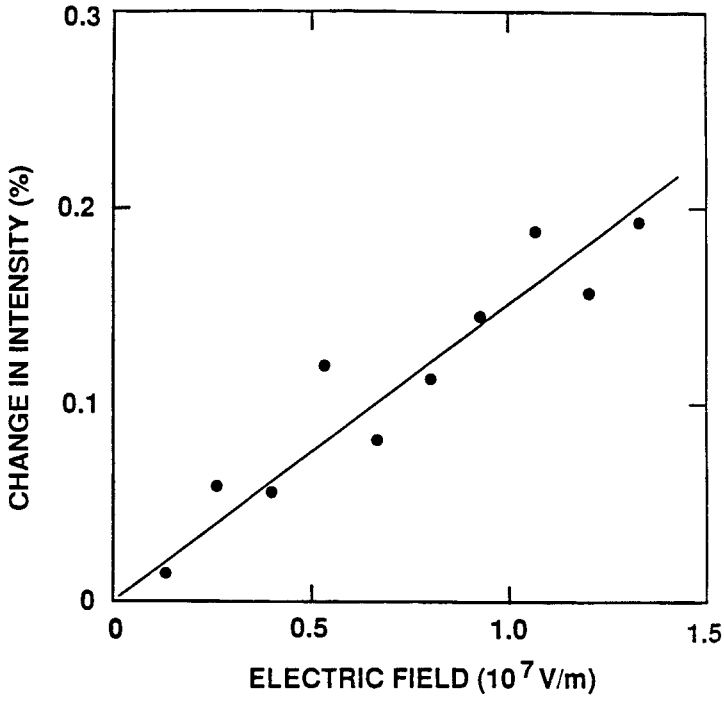

Figure 26. The change in intensity of a diffracted X-ray beam as a function of an applied electric field. The straight line is a least-squares fit to the data constrained to go through the origin. (From Kepler *et al.* [149].)

crystallinity, that is $\gamma = 0{\cdot}33$, equation (41) predicts that the field dependence of crystallinity should be $2{\cdot}76 \times 10^{-11}\,V^{-1}\,m$. The experimentally observed value, obtained from the data in figure 26, is $1{\cdot}8 \times 10^{-10}\,V^{-1}\,m$, more than six times larger. The effective observed change is crystallinity would therefore predict a pyroelectric coefficient considerably larger than the value that we have used. The effect is clearly large enough to support the hypothesis that reversible changes in crystallinity contribute significantly to the pyroelectric coefficient. A likely reason for the discrepancy is an overestimated value of the latent heat at 298 K. Alternatively, melting of crystallites may not result in complete disorientation of the dipole moments of the monomer units.

Clements *et al.* [152] have estimated the reversible change in crystallinity between 20 and 60°C for PVF_2 from nuclear-magnetic resonance (NMR) measurements. In broad-line NMR measurements the spectra shows two component lines with distinctly different linewidths. The broad component was assigned to the crystalline regions of the polymer and the narrow component to an oriented non-crystalline phase. By measuring the intensity of the two lines as a function of temperature they found that the crystalline fraction dropped from 0·503 to 0·427 over the temperature range 20–60°C for a uniaxially oriented sample. If the dipole moments of all the material which leaves the crystalline phase become randomly oriented, these results would predict a pyroelectric coefficient of $-25 \times 10^{-5}\,C\,m^{-2}\,K^{-1}$ if the polarization of the crystalline phase is $0{\cdot}013\,C\,m^{-2}$. The experimentally measured value of the pyroelectric coefficient

is about ten times smaller and therefore reversible changes in crystallinity are again predicted to produce a much larger pyroelectric coefficient than is observed experimentally.

Dvey-Aharon *et al.* [153] have considered reversible changes in crystallinity in PVF_2 from a theoretical point of view. Their model predicts contributions from this effect which are massively larger than is required to explain the experimental observation.

In view of the extensive experimental and theoretical evidence, it is now well established that reversible changes in crystallinity with temperature is an important effect. In fact the evidence suggests that its contribution should be larger than is observed. The problem now is to explain why the contribution from reversible changes in crystallinity is so small. Perhaps the dipoles leaving the crystalline phase remain oriented to a large extent.

2.4.2.4. *Theoretical models.* Attempts to model the pyroelectric effect in PVF_2 theoretically were first made by Aslaksen [52]. His model was based on the fact that the average dipole moment depends on the amplitude of libration of the monomer dipoles and that the amplitude of libration increases with increasing temperature. Hayakawa and Wada [19, 154] and Wada [155, 156] proposed that trapped charge is an important contributor and have investigated that hypothesis in some detail. In general, trapped charge will only contribute if mechanical inhomogeneities are present and it is now thought that any contribution from trapped charge is small. Broadhurst *et al.* [157] pointed out that rigid dipoles would produce pyroelectricity simply because the number of dipoles per unit volume would change with temperature, and Mopsik and Broadhurst [78] improved on this model by including two additional effects. The dipoles were allowed to be polarizable and thus the dipole moment depended on the local field, and the dipoles were assumed to librate about their equilibrium orientations with a temperature-dependent amplitude. An Onsager [76] cavity approach was used to calculate the local field but the result is the same as that obtained by using the Lorentz field approximation [77] as was discussed earlier in this review in the section on remanent polarization. The Clausius–Mossotti relation, which is derived in the Lorentz field approximation, was used to determine the polarizability of the dipoles. The mean squared amplitude of libration of the dipoles was assumed to be that for a classical harmonic oscillator:

$$\langle \phi_0^2 \rangle = \frac{2k_B T}{I\omega^2}, \tag{42}$$

where I is the moment of inertia and ω is the frequency. The average contribution of the dipoles $\langle \cos \theta_0 \rangle$, with θ_0 being the angle between the film normal and the orientation of the dipole, to the sample moment was treated as an adjustable parameter.

The model of Broadhurst *et al.* [157] was developed for homogeneous electrets but it was subsequently extended to be applicable to semicrystalline polymers such as PVF_2 [75]. The effects of compensating charge at the crystallite surfaces, the lamellar morphology and the presence of the amorphous phase were all included. Broadhurst *et al.* concluded that the agreement between their theory and experiment was good to within 20% and that the largest contribution to the pyroelectric coefficient arises from the bulk dimensional changes (50%) compared with 23% from changes in molecular dipole fluctuations and 27% from changes in the local field. This model was based on

the Lorentz local field approximation but the very high remanent polarization for a single crystal, 0·020–0·022 C m^{-2}, which it predicts did not enter into the comparison of the results of this model with experiment. Experimentally determined remanent polarizations were used because the orientation distribution of the dipole moments of the crystalline regions relative to the film surface was not known.

The prediction that 23% of the pyroelectric response results from dipole libration is interesting in the light of experimental results [144] which led to the conclusion that no evidence could be seen for a primary contribution to the pyroelectric coefficient and that, if one did exist, it would have to be less than 15%. In the theory of Broadhurst *et al.*, there are two parts to the dipole libration term: one which results simply from the change in temperature and another which arises from the change in sample dimension when the temperature is changed. The first contribution would be primary pyroelectricity and the magnitude of this contribution is predicted to be 15%. If the 200 ps pulse heating experiment can be done with better precision, it might detect the change in libration amplitude which results simply from a change in temperature, and thus a primary pyroelectric contribution.

Purvis and Taylor [81, 158] and Al-Jishi and Taylor [83] have calculated the pyroelectric coefficient they would expect from their model, in which the local field was calculated taking the orthorhombic crystal structure into account. They assumed that the mechanical properties of stretch oriented PVF_2 films measured by Ohigashi [159] at temperatures well below the glass transition temperature were the properties of single crystals and that the only role of the amorphous phase was to transfer stress and change dimensions with temperature. They found that the contribution from the change in the local field was larger than the contribution from the change in dimensions and that, even though their model was quite simple, the calculated pyroelectric coefficient was in reasonable agreement with experimental results. They did not consider the effect of dipole libration.

2.4.2.5. *Summary.* A comprehensive understanding of pyroelectricity in PVF_2 remains elusive. There is not a shortage of effects that might adequately explain the experimental observations but the accuracy of the theoretical calculations do not allow an adequate test of the various hypotheses. Clearly the effect of sample dimensions and of the polarization of the dipoles by the local field are important effects. It is not clear that the effect of molecular librations needs to be considered. A large number of observations have shown that reversible changes with temperature of the sample crystallinity are playing a very important role and the problem with this mechanism is explaining why its contribution is not larger. PVF_2 samples are so complex and there are so many adjustable parameters that it seems unlikely that much more progress can be made towards separating the various contributions theoretically. Clever experiments are needed.

2.4.3. *Piezoelectricity*

2.4.3.1. *Measurement techniques.* There are potentially 18 coefficients in the piezoelectric coefficient matrix d_{im} but the overall mm2 orthorhombic symmetry typical of a highly oriented poled polymer film reduces the number of independent coefficients to five. In the usual convention where 1 is parallel to the draw direction, 2 is in the plane of the film and perpendicular to the draw direction and 3 is perpendicular to the film surface, they are d_{31}, d_{32}, d_{33}, d_{15} and d_{24}. If the film is poled and biaxially oriented or unoriented, $d_{31}=d_{32}$ and $d_{15}=d_{24}$.

The easiest way to measure d_{31} and d_{32} is to prepare long thin samples with electrodes on opposite sides, to attach one end to a rigid support, and to attach a small weight to the other end [140]. Then, with an electrometer connected between the electrodes, the charge induced on the electrodes should be measured when a small additional weight is added to the lower end.

Extensive use has been made, particularly in Japan, of a technique originally developed by Fukuda *et al.* [160]. Thin films are mounted in an apparatus which holds the sample under tension and the longitudinal stress on the sample is varied sinusoidally. The stress or strain and charge output from electrodes on opposite sides of the thin-film sample are measured simultaneously. Generally it is found that in polymers the piezoelectric charge signal is not in phase with the stress or strain, presumably because the polymers are viscoelastic, but the phase difference may result from stress-induced reversible changes in crystallinity which lag behind the application of stress. It has been proposed that reversible stress-induced changes in crystallinity contribute significantly to the piezoelectric coefficient in PVF_2 [153]. Because of the phase difference the piezoelectric coefficients are found to be complex quantities. Both the frequency and the temperature dependences can be readily measured using the technique, and many studies of piezoelectricity in a wide variety of polymers have been reported.

Typically the electrodes on the polymer samples are very thin evaporated metal films. In order not to introduce errors, it is necessary to keep the electrodes thin enough that they do not perturb the mechanical properties of the sample.

Ohigashi [159], Bui *et al.* [161] and Schewe [162] have made measurements of the piezoelectric coefficients at high frequencies using piezoelectric resonances. Schewe has carried out a particularly complete set of measurements including dielectric and mechanical as well as piezoelectric experiments. His most complete set of measurements were made using the quasi-static technique described above, at 10 Hz, but length extensional and thickness resonances at 25 kHz and 41 MHz respectively were also studied. The resonance technique consists of measuring the impedance of a freely vibrating piezoelectric element as a function of frequency near a resonance. The variation in the impedance with frequency is determined by the sample elastic constants, the acoustic loss factor Q and the electromechanical coupling coefficients.

In the piezoelectric resonance technique the electromechanical coupling coefficients are

$$k_{ij}^2=\frac{(\kappa_{ij}^{\sigma}-\kappa_{ij}^{\varepsilon})}{\kappa_{ij}^{\sigma}}, \tag{43}$$

where $\kappa_{ij}^{\varepsilon}$ is the clamped dielectric permittivity, that is the permittivity observed when the dimensions of the sample are held constant, and κ_{ij}^{σ} is the free dielectric permittivity. The relation between the electromechanical coupling coefficients and the piezoelectric coefficients is derived from the following relations, or some variation of them:

$$\mathrm{d}D_i=\kappa_{ij}^{\sigma}\,\mathrm{d}E_j+d_{ijk}\,\mathrm{d}\sigma_{jk}, \tag{44}$$

$$\mathrm{d}\varepsilon_{ij}=s_{ijkl}\,\mathrm{d}\sigma_{kl}+d_{ijk}\,\mathrm{d}E_k, \tag{45}$$

and it is assumed that the direct and converse piezoelectric coefficients are equal. As will be discussed in the next section, we have shown both theoretically and experimentally that they are not equal [136] and in the case of low-modulus materials such as polymers the error from the assumption of equality can become large. As we discussed

in a previous review [20] and shall show later in this review, the equation that should be used instead of equation (44) is

$$dD_i = \kappa_{ij}^{\sigma} dE_j + \left(d_{ijk} - \frac{P_i}{A_i} \frac{\partial A_i}{\partial \sigma_{jk}} \right) d\sigma_{jk}. \tag{46}$$

With the aid of matrix notation and a one-dimensional approximation [159], equations (45) and (46) lead to

$$k_{31}^2 = \frac{d_{31}^2 c}{\kappa_3^{\sigma}} \left(1 - \frac{1}{d_{31}} \frac{P}{A} \frac{\partial A_i}{\partial S_{jk}} \right) \tag{47}$$

rather than

$$k_{31}^2 = \frac{d_{31}^2 c}{\kappa_3^{\sigma}}, \tag{48}$$

as is obtained from equations (44) and (45). In these equations, c is the elastic stiffness. To show how important this correction can be, Ohigashi calculated a value of $30{\cdot}7\,\mathrm{pC\,N^{-1}}$ for d_{31} in PVF_2 from a measured value for k_{31} of 0·151. When we recalculated d_{31} using equation (47) and the values for c and κ^{σ} given by Ohigashi and by assuming that the polarization was $5 \times 10^{-2}\,\mathrm{C\,m^{-2}}$ and that $A^{-1}(\partial A/\partial\sigma) = 2{\cdot}43 \times 10^{-10}\,\mathrm{Pa^{-1}}$, we obtained [20] $37\,\mathrm{pC\,N^{-1}}$. As we shall show later the correction can even be much greater in some cases. The error introduced by the one-dimensional assumption does not seem to have been investigated.

Rezvani and Linvill [163] have developed an all-electrical technique for the measurement of piezoelectric parameters of PVF_2. A thin polymer film with thin evaporated-metal electrodes on each side is held under slight tension between two rigid supports. The metal electrode on one side is etched away in the middle to form two separate electrodes, one on each end. A voltage applied between one of the electrodes and the electrode on the opposite side develops a stress in the film which in turn changes the voltage between the second electrode and the electrode on the opposite side. The piezoelectric coefficient d_{31} was then calculated from the relation

$$d_{31} = \frac{2v_2}{v_1} \frac{\kappa^{\sigma}}{c^E} \tag{49}$$

where v_1 is the applied voltage, v_2 the measured voltage, κ^{σ} the dielectric constant under constant stress and c^E Young's modulus of the film under constant electric field. This technique allowed them to study the effect of high d.c. bias fields on the piezoelectric coefficient d_{31}.

The piezoelecric coefficient d_{33} is very difficult to measure without constraining the sample in its lateral dimensions. Kepler and Anderson [140] measured the converse piezoelectric coefficient d_{33}^{c} by suspending an electroded sample between two needles, one rigidly attached to a substrate and the other free to move as the sample thickness changed. The needles both held the sample in place and provided electrical contact to the electrodes. The change in thickness was measured by mounting a mirror on the needle which was free to move and by measuring its displacement with applied field using a laser interferometer technique.

A more commonly used technique to determine d_{33} is to measure the hydrostatic piezoelectric coefficient d_{3h} by measuring the change in charge on a sample as a function of hydrostatic pressure and then to calculate d_{33} from the relation

$$d_{3h} = d_{31} + d_{32} + d_{33}. \tag{50}$$

The results obtained by Kepler and Anderson [140] are shown in table 1.

Nix and Ward [164] have developed a technique for the measurement of the shear piezoelectric coefficients. They glued uniaxially oriented PVD_2 sheets between blocks of Perspex and attached electrodes on the edges of the sample perpendicular to the 1 direction and to the 2 direction. When the sample and blocks of Perspex were mounted in an appropriate rig, a simple shear could be applied in the 1–3 plane and the change in polarization detected by the electrodes perpendicular to the 1 direction to determine d_{15}. Similarly, shear in the 2–3 plane and detection of the change in polarization with the electrode mounted perpendicular to the 2 direction gives d_{24}.

2.4.3.2. *Direct versus converse piezoelectric coefficients.* As was mentioned previously, it is usually stated that the direct and converse piezoelectric coefficients, d_{ij} and d^c_{ij} respectively, are equal [10, 12, 137, 165]. PVF_2 provided an opportunity to test this statement since long strips with electrodes on both sides could be prepared. With one end attached to a rigid support and a small weight attached to the other to hold it vertical, both the direct and the converse coefficients could be measured, the direct by adding weight and measuring the change in charge on the electrodes and the converse by applying a voltage between the two electrodes and measuring the change in length. These experiments were undertaken by Kepler and Anderson [140] and they obtained the very surprising result that $\partial\varepsilon/\partial E = A^{-1}(\partial Q/\partial\sigma)$ within a few per cent. However, if the data were corrected to obtain the direct piezoelectric coefficient $\partial P/\partial\sigma$, that is

$$\frac{\partial P}{\partial\sigma} = \frac{1}{A}\frac{\partial Q}{\partial\sigma} - \frac{P}{A}\frac{\partial A}{\partial\sigma}, \tag{51}$$

a very large discrepancy developed. The experimentally measured $d_{31} = A^{-1}(\partial Q/\partial\sigma)$ was $+4{\cdot}3\,\mathrm{pC\,N^{-1}}$ while the correction $(P/A)(\partial A/\partial\sigma)$ was calculated to be $-12{\cdot}1\,\mathrm{pC\,N^{-1}}$ and thus $\partial P/\partial\sigma = -7{\cdot}8\,\mathrm{pC\,N^{-1}}$.

This observation lead to a re-examination of the derivation of the relation between the direct and converse piezoelectric coefficients [136, 140]. The general statement is that

$$\left.\frac{\partial P_i}{\partial\sigma_{jk}}\right|_{E,T} = \left.\frac{\partial\varepsilon_{jk}}{\partial E_i}\right|_{\sigma,T}. \tag{52}$$

This equation is one of a class of thermodynamics equations known as the Maxwell relations which are derived from various thermodynamic potentials by using the fact that the value of mixed second derivatives, $\partial^2\phi/\partial x\,\partial y$, is independent of the order of differentiation. The thermodynamic potentials are derived for piezoelectric materials by using $\mathrm{d}W_\sigma = \sigma_{jk}\,\mathrm{d}\varepsilon_{jk}$ for the amount of work done by stress and $\mathrm{d}W_E = E_i\,\mathrm{d}D_i$ for the amount of work done by the electric field. Then with s and u here denoting the entropy and energy densities (rather than the molar quantities), the change in internal energy density is

$$\mathrm{d}u = \sigma_{jk}\,\mathrm{d}\varepsilon_{jk} + E_j\,\mathrm{d}D_i + T\,\mathrm{d}s. \tag{53}$$

Then, if a thermodynamic potential is defined as

$$\phi = \sigma\varepsilon + ED + Ts - u, \tag{54}$$

$$\mathrm{d}\phi = \varepsilon_{jk}\,\mathrm{d}\sigma_{jk} + D_i\,\mathrm{d}E_i + s\,\mathrm{d}T \tag{55}$$

and

$$\left.\frac{\partial\phi}{\partial\sigma_{jk}}\right|_{E,T} = \varepsilon_{jk}, \quad \left.\frac{\partial\phi}{\partial E_i}\right|_{\sigma,T} = D_i. \tag{56}$$

Taking the second partial derivatives with respect to the opposite variables leads to equation (52) at $E=0$ since $D=\kappa_0 E+P$.

There is a problem with this derivation in that the use of reduced variables σ, ε, E and D does not take into account the important effect of changes in sample dimensions, because $dW_E=E_i\,dD_i$ is true in general only if the sample dimensions do not change [151]. To correct this problem the Maxwell relations were rederived [136, 140] using F, x, V and Q as the variables rather than the normalized quantities, where F is the total force applied to the sample, dx is the distance over with the force F is applied, V is the the voltage applied across the electrodes and dQ is the change in the total free charge on the electrodes. This derivation assumes that the electrodes expand and contract with the sample.

Following the procedure used in equations (53)–(56) a Maxwell relation similar to equation (52) is obtained [136, 140]:

$$\left.\frac{\partial Q}{\partial F}\right|_{V,T}=\left.\frac{\partial x}{\partial V}\right|_{F,T}, \tag{57}$$

and this equation was converted to reduced variables by using the relations $F_{jk}=A_j\sigma_{jk}$, $x_{jk}=l_j\varepsilon_{jk}$, $V_i=l_iE_i$ and $Q_i=A_iP_i$ where A and l are the areas and lengths required to give the correct total quantity. In differentials such as

$$dF_{jk}=A_j\,d\sigma_{jk}+\sigma_{jk}\,dA_j,$$

the second term on the right-hand side vanishes at zero stress or electric field and can therefore be neglected but, for the charge

$$dQ_i=A_i\,dP_i+P_i\,dA_i,$$

both terms on the right must be kept because in ferroelectrics the polarization does not go to zero as V goes to zero. Then the correct relation between the direct and converse piezoelectric coefficients is found to be [136, 140]

$$\left.\frac{\partial P_i}{\partial\sigma_{jk}}\right|_{E,T}+\frac{P_i}{A_i}\left.\frac{\partial A_i}{\partial\sigma_{jk}}\right|_{E,T}=\left.\frac{\partial\varepsilon_{jk}}{\partial E_i}\right|_{\sigma,T}. \tag{58}$$

Other Maxwell relations for ferroelectrics are affected in the same way if differentials of the polarization are involved. For example, it is usually stated that

$$\left.\frac{\partial P_i}{\partial T}\right|_{\sigma,E}=\left.\frac{\partial s}{\partial E_i}\right|_{\sigma,T} \tag{59}$$

where $\partial s/\partial E$ is the electrocaloric coefficient but the procedure used above shows [136] that the correct relationship between the pyroelectric coefficient and the electrocaloric coefficient is

$$\left.\frac{\partial P_1}{\partial T}\right|_{\sigma,E}+\frac{P_i}{A_i}\left.\frac{\partial A_i}{\partial T}\right|_{\sigma,E}=\left.\frac{\partial s}{\partial E_i}\right|_{\sigma,T}. \tag{60}$$

There are experimental results [166] which show that equation (60) is correct rather than equation (59) just as the experimental results [140] discussed above show that equation (58) is correct.

It is of some interest to speculate why these discrepancies had not been discovered earlier. The reason is probably related to the mechanical properties of the more familiar

ferroelectric materials which are much less elastically compliant than PVF_2. For ferroelectric ceramics the error in equation (52) is only of the order 10% whereas, as shown above, the correction term can be dominant in PVF_2.

2.4.3.3. *Experimental results.* The data on mechanical properties and piezoelectric coefficients of PVF_2 obtained by Schewe [162] at ambient temperature and at three different frequencies are shown in table 2 and can be compared with similar data obtained static measurements [140] presented previously in table 1. All the data presented in the tables are the uncorrected or experimental values.

Humphreys *et al.* [167, 168] undertook an investigation of the effect of processing conditions on the mechanical properties and on the three piezoelectric coefficients d_{31}, d_{33} and d_{3h}. From their studies they concluded [168] that piezoelectricity results from a number of mechanisms and that dimensional changes is one of them but not necessarily the most important.

A complete set of direct piezoelectric coefficients, including the shear coefficients which were measured using the technique described in section 2.4.3.1, have been reported by Nix and Ward [164]. For d_{15} the values that they reported range from $-13{\cdot}1$ to $-27\,pC\,N^{-1}$ and for d_{24} from -23 to $-38{\cdot}3\,pC\,N^{-1}$ for differently processed films.

Table 2. Mechanical, dielectric and piezoelectric properties of PVF_2. (From Schewe [162].) v_{ij} and e_{ij} are the Poisson ratios and stress piezoelectric coefficients respectively.

	Value at the following frequencies		
Material parameters	10 Hz	25 kHz	41 MHz
d_{31} ($pC\,N^{-1}$)	28	17·5	
d_{32} ($pC\,N^{-1}$)	4	3·2	
d_{33} ($pC\,N^{-1}$)	−35		
d_h ($pC\,N^{-1}$)	−3		
e_{31} ($10^{-3}\,C\,m^{-2}$)	42		
e_{32} ($10^{-3}\,C\,m^{-2}$)	−6		
e_{33} ($10^{-3}\,C\,m^{-2}$)	−59		−90·2
s_{11} ($10^{-10}\,Pa^{-1}$)	3·65	2·49	
s_{22} ($10^{-10}\,Pa^{-1}$)	4·24	2·54	
s_{33} ($10^{-10}\,Pa^{-1}$)	4·72		
s_{12} ($10^{-10}\,Pa^{-1}$)	−1·10		
s_{13} ($10^{-10}\,Pa^{-1}$)	−2·09		
s_{23} ($10^{-10}\,Pa^{-1}$)	−1·92		
c_{33} (10^9 Pa)	5·4		9·55
v_{21}	0·25		
v_{31}	0·57		
v_{32}	0·45		
κ_{33}	15	13·6	4·9
$\tan\delta$		0·06	0·22
k_{31} (%)	13	10·2	
k_{32} (%)	1·7	1·8	
k_t (%)			14·4

Wang [169] and Yagi *et al.* [170] have studied the effect of rolling as well as drawing. As discussed in section 2.3.3, rolling produces increased orientation of the *a* and *b* axes of the unit cell, tending to orient the *a* axis in the plane of the film. Wang [169] found that, in the drawn and rolled films, d_{31} tended to be about 25% higher than in films that had only been drawn. Yagi *et al.* [160] have found that d_{31} can be as large as $49\,\mathrm{pC\,N^{-1}}$ in rolled films of a 52 mol% VDF–48 mol% F_3E copolymer. The remanent polarization of these films was $0{\cdot}102\,\mathrm{C\,m^{-2}}$.

It has also been shown that annealing can have a large effect on the magnitude of the piezoelectric coefficients. Takase *et al.* [71] have found that annealing stretched PVF_2 films at temperatures between 160 and 180°C has a marked effect on the magnitude of the piezoelectric coefficients and remanent polarization. In the samples studied, d_{31} increased from 20 to $28\,\mathrm{pC\,N^{-1}}$ and the remanent polarization from 0·056 to 0·085 $\mathrm{C\,m^{-2}}$. Ohigashi *et al.* [40] have found that thick lamellar single crystals and large bulk single crystals grow in films of VDF–F_3E copolymers when they are annealed at temperatures between the Curie temperature and the melting point and Ohigashi and Hattori [41] have observed lamellar crystals of PVF_2 about 0·2 μm thick and 10 μm wide in films that were crystallized at high pressures (2–5 kbar) and high temperatures (260–300°C). The piezoelectric coefficients were not reported but the crystal structure was β-phase and the remanent polarization of the PVF_2 films was found to be $0{\cdot}1\,\mathrm{C\,m^{-2}}$.

It is now well established that the magnitude of the piezoelectric coefficients depend on the remanent polarization. The relationship is linear in PVF_2 [142] but nonlinear in VDF–F_3E copolymers [142, 171, 172]. The nonlinearity is attributed to the fact that the VDF–F_3E copolymers undergo extensive mechanical hardening during poling [142]. The relationship between the remanent polarization and d_{31} divided by Young's modulus is linear in these copolymers [142].

The temperature dependence of the piezoelectric coefficients has been investigated by several groups [48, 88, 159, 173–175]. In general it is found that the piezoelectric coefficients increase with increasing temperature, increasing more rapidly above the glass transition temperature which is in the vicinity of −50°C. Some results obtained by Ohigashi [159] for the temperature dependence of the piezoelectric strain d_{ij} and stress e_{ij} coefficients are shown in figure 27.

2.4.3.4. *Theoretical models.* The situation with regard to theoretical models for piezoelectricity appears to be somewhat clearer than for pyroelectricity. There are basically two effects that need to be considered to explain the experimental results within the accuracy of the experimental data. One is simply the sample dimension effect. If the dipole moment and number of the dipoles are kept constant, piezoelectricity can be produced when the sample dimensions are changed. The other is the effect of the local field on the magnitude of the dipole moment.

Broadhurst *et al.* [75], as discussed previously, proposed a model that included these two effects as well as dipole libration and space charge effects. The Lorentz approximation was used to determine the local field and the dipole polarizability. Within their model they only calculated the hydrostatic piezoelectric coefficient and concluded that 37% of the experimentally measured coefficient arose from the local field effect, 10% from dipole fluctuations and 60% from dimensional changes. The model predicted a slightly larger coefficient than observed experimentally. Purvis and Taylor [81, 158] have calculated the piezoelectric coefficients that are predicted by their point dipole and orthorhombic lattice model for the local field. They did not

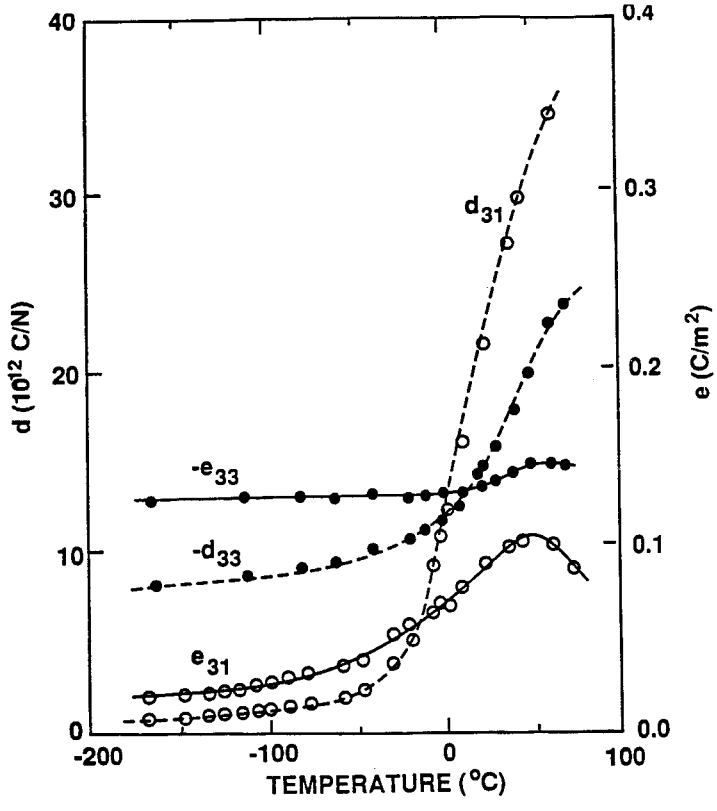

Figure 27. Temperature dependence of the piezoelectric strain coefficients d_{31} and d_{33}, and of the piezoelectric stress coefficients e_{31} and e_{33}, as determined by Ohigashi [159] for films of PVF_2.

consider dipole libration or space charge effects but were able to obtain quite good agreement with experimental values including d_{31} and d_{32}. Then Al-Jishi and Taylor [83] extended the calculations of Purvis and Taylor [81] to include a better approximation for the dipoles, one in which the dipoles were represented by separated charge [82]. This model, as well as the others, was discussed previously in both section 2.4.2 and section 2.3.2 and is the one which agrees best with the remanent polarization experimental results. The predictions of these three models and experimental results are presented in table 3.

Tashiro *et al.* [176] have shown that the variations in the monomer dipole moment and the dielectric constants of both the crystalline and the amorphous regions with applied stress are effects that should be considered. Al-Jishi and Taylor [83] believe that, if they had included these effects in their model, it would have improved the agreement between theory and experiment.

Dvey-Aharon *et al.* [153] have considered the possibility that reversible changes in crystallinity with stress might play a role in piezoelectricity. Ohigashi [159] has suggested that stress applied parallel to the long axis of the polymer molecules might reduce the steric hindrance that causes the statistical displacement of the fluorine groups along the molecule, thus increasing the effective dipole moment and contributing to the piezoelectric effect. Wada and Hayakawa [177] have considered a model involving spontaneously polarized spheres embedded in a matrix.

Table 3. Predictions for the magnitude of the piezoelectric and pyroelectric coefficients by various models compared with experimental results.

Coefficient	Value according to the theoretical models			
	Broadhurst *et al.*[a]	Purvis and Taylor	Al-Jishi and Taylor	Experiment[b]
d_{31} (pC N^{-1})		18·1	15·0	21·4
d_{32} (pC N^{-1})		4·8	4·8	2·3
d_{33} (pC N^{-1})		−28·9	−29·3	−31·5
d_h (pC N^{-1})	−12·9	−6·2	−9·3	−9·6
p_3 (10^{-5} C m^{-2} K^{-1})	−2·5	−2·4	−2·8	−2·74

[a] Assuming that the remanent polarization is 0·06 C m^{-2}.
[b] From Kepler and Anderson [140].

2.4.3.5. *Summary.* PVF_2 exhibits large piezoelectric effects which appear to arise from primarily two effects: changes with stress in sample dimensions which change the number of dipoles per unit volume, and changes in the local field which change the magnitude of the monomer dipole moment. Several other mechanisms which probably contribute to the piezoelectricity have been identified but experimental evidence that they are important does not yet exist. Tests of the Maxwell relation between the direct and converse piezoelectric coefficients have shown that they are not equal as is commonly believed and the correct relationship has been derived.

2.5. *Nonlinear optical properties*

Second-harmonic generation of light at 532 nm in thin films of PVF_2 was studied by Bergman *et al.* [6] and McFee *et al.* [8] shortly after Kawai [5] reported that he had observed a large piezoelectric effect. They cut wedge-shaped samples from stretch oriented film sheets 19 μm thick and mounted them in an index-matching fluid to minimize scattering and reflection losses at the edges of the wedges where the light entered the sample. The wedges were cut to taper from 0·015 to 0·005 in. The light from a neodymium-doped yttrium aluminium garnet laser ($\lambda = 1{\cdot}06$ μm) with a peak power of about 100 W was incident on the edge of the film so that the beam propagated in the plane of the film and was focused so that its waist was contained in the film. Wedges were cut in two orientations, with the length parallel to the 1 or draw direction and with the length perpendicular to the draw direction. The 3 direction, the direction in which the dipoles were oriented, was always perpendicular to the plane of the wedge.

In the mm2 symmetry of stretch oriented and poled PVF_2 films, there are three independent second-order nonlinear coefficients and the components of the second-harmonic polarization are given in terms of the electric field components of the incident light by [8]

$$P_1 = 2\delta_{31} E_1 E_3, \tag{61}$$

$$P_2 = 2\delta_{32} E_2 E_3, \tag{62}$$

$$P_3 = \delta_{31} E_{12} + \delta_{32} E_{22} + \delta_{33} E_{32}. \tag{63}$$

When the incident light was propagating parallel to the molecular axis, the 1 direction, second-harmonic light polarized in the 3 direction was observed if the

polarization of the incident light was in either the 2 or the 3 direction as predicted by equations (61)–(63). If the wedge was cut so that the light propagated in the plane of the film and parallel to the 2 direction, perpendicular to the chain axis, and the polarization of the incident beam was parallel to the 1 direction, no second-harmonic light was observed, indicating that δ_{32} is very small compared with δ_{31} and δ_{33}.

When the wedge was translated parallel to its length, the length of the light path in the sample changed and an oscillatory behaviour in the intensity of the second harmonic was observed. Such interference fringes result from phase matching between the fundamental and second harmonic and a coherence length of about 30 μm was determined from the fringe spacing. By comparing the intensity of the second-harmonic signal generated in the polymer with that generated in a quartz crystal wedge the magnitude of the nonlinear optical coefficients of PVF_2 relative to that of quartz was found to be

$$\delta_{33}(PVF_2) \approx 2\delta_{31}(PVF_2) \approx \delta_{11}(SiO_2),$$

$$\delta_{32}(PVF_2) \approx 0.$$

Using a very similar experimental set-up, Sato and Gamo [178] have observed second-harmonic generation at 532 nm in a film of a 78 mol% VDF–22 mol% F_3E copolymer. They reported a coherence length of 200 μm. Wicker *et al.* [179] have also reported observation of second-harmonic generation in a 70 mol% VDF–30 mol% F_3E. In their experiment the light was incident normally on the film and with transparent electrodes the magnitude of the second harmonic signal could be measured as a function of the applied field. The magnitude of the signal varied as expected as the direction of polarization was reversed.

3. Other ferroelectric polymers

3.1. *Ferroelectric liquid-crystalline polymers*

In 1975, Meyer *et al.* [180] showed by symmetry arguments that chiral smectic C liquid crystals would be ferroelectric. Liquid crystals consist of rod-like molecules in some sort of ordered structure. In the nematic phase, the lowest-order structure, the long axis of the molecules are aligned but in addition the molecules are arranged in a layered structure.

In the smectic C-phase the molecules are tilted relative to the normal to the plane of the layers and are in an environment with monoclinic symmetry. The general monoclinic cell contains three symmetry elements: a two-fold axis normal to the long axis of the molecule and in the plane of the layer, a mirror plane normal to the twofold axis and a centre of inversion. If the molecule is chiral (not superposable on its mirror image), the mirror plane and centre of inversion are eliminated and the structure can have a spontaneous polarization. Typical liquid-crystalline molecules have a permanent dipole moment and, if they are chiral, there must be a component parallel to the twofold axis in the smectic C-phase. In macroscopic samples the molecular tilt direction precesses around the normal to the layers in a helicoidal structure with a pitch of several microns and a macroscopic polarization is not observed unless the sample is thin relative to the pitch of the helix or an electric field is applied to increase the pitch.

In collaboration with chemists, Meyer [180] also prepared a ferroelectric liquid crystal and demonstrated that it was indeed ferroelectric. The molecule was *p*-decyloxybenzylidene-p′-amino-2-methylbutyl cinnamate.

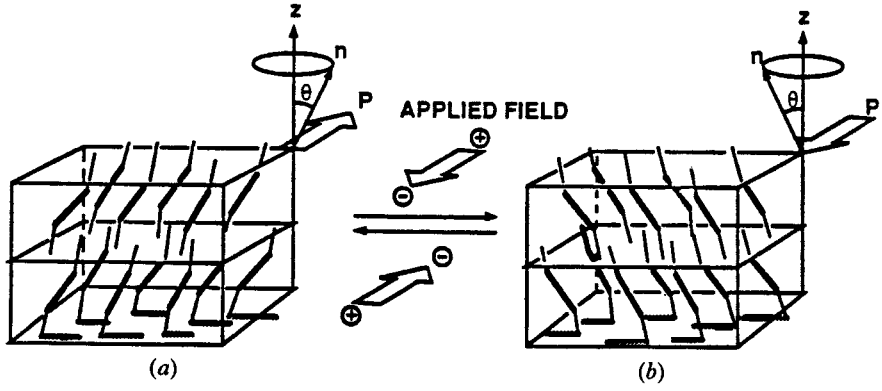

Figure 28. Principle of operation of the surface-stabilized ferroelectric liquid-crystalline light valve. The cell, represented schematically in (*a*), is placed between crossed polarizers and the incident light propagates parallel to the direction of the applied field. If the plane of polarization of the incident light is parallel to the vector ***n***, all the light is stopped. If the direction of the applied field is reversed, thereby changing the orientation of the molecules, as indicated in (*b*), the birefringence of the cell changes the polarization of the incident light, allowing some to be transmitted through the second polarizer (Adapted from Walba and Clark [205].)

The remanent polarization is generally quite small for liquid crystals for two reasons. First, the coupling of the molecule to the monoclinic environment tends to be weak so that the molecule can rotate about its long axis and, second, if the chiral part of the molecule is only weakly coupled to the polar part, the internal molecular rotations reduce the average dipole moment.

In 1980, Clark and Lagerwall [181] demonstrated that it is possible to develop a fast-switching electro-optical device using ferroelectric liquid crystals and the number of papers in the area has increased rapidly ever since. They demonstrated that surface interactions can be used to suppress the formation of the helical structure in a geometry that allowed the stabilization of two domains of opposite polarization, fast switching between the two states by applying an electric field, and a large index of refraction anisotropy which rotated through a large angle when the states were switched. Thus, when such a cell with transparent electrodes was placed between crossed polarizers, it became a fast electro-optic switch. The principle of operation of their device is illustrated in figure 28.

The work on ferroelectric liquid crystals led naturally to attempts to synthesize ferroelectric side-chain liquid-crystalline polymers, polymer backbones with chiral smectic C-phase forming molecules attached as side chains. The first to do so was Shibaev and co-workers [182, 183]. The molecule they synthesized was I:

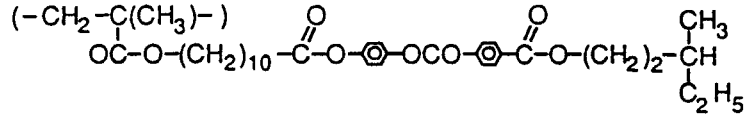

I

Many such polymers have now been synthesized but very little is yet known about their physical properties. A review which emphasizes synthesis and a summary of the molecules which have been synthesized has been published by Le Barny and Dubois [184].

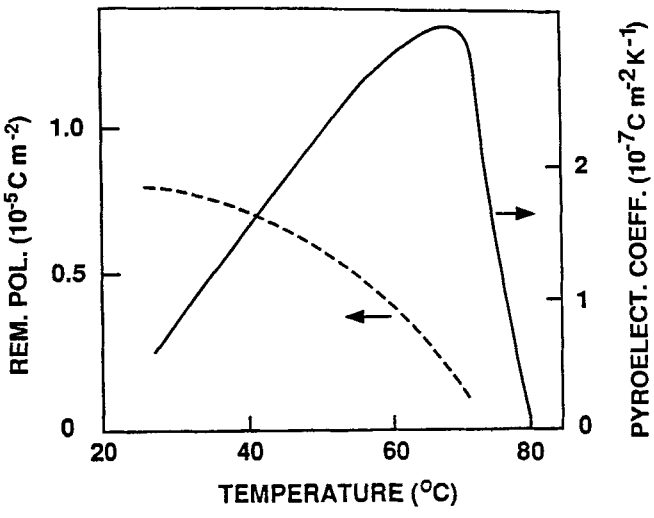

Figure 29. Temperature dependence of the remanent polarization and the pyroelectric coefficient of the ferroelectric side chain polymer *I*. (From Shibaev and Plate [183].)

The remanent polarization of I as a function of temperature is shown in figure 29. The field required to switch the direction of polarization in the polymer, which is presumably closely related to the coercive field, is very low [185], 0·3 MV m^{-1}.

Scherowsky *et al.* [186] have shown that the switching time of one of the polymers which they have synthesized, a polyacrylate, varies inversely with the applied electric field. This behaviour is typical of ferroelectric liquid crystals and has been modelled by assuming that the rod-like molecules are rotating in a viscous fluid under the torque applied by the interaction of the electric field and the dipole moment of the molecule [187].

Remanent polarizations are still low compared with the 0·1 C m^{-2} of PVF_2 but they appear to be increasing as more molecules are synthesized. The highest we found was that reported by Kapitza *et al.* [188] for a polysiloxane, 0·0043 C m^{-2}.

The observation of ferroelectric modes by dielectric spectroscopy in a polymer in which both the backbone and the side chains form liquid crystals has been reported by Vallerien *et al.* [189]. Only the side chains form the ferroelectric phase.

A variety of possible applications are driving the development of these materials and a number of them are different from those envisaged for either PVF_2 or low-molecular-weight ferroelectric liquid crystals. For example, considerable effort is at present being expended in attempts to prepare molecularly doped polymers in which non-centrosymmetric molecules can be oriented for second-order nonlinear optical device applications. It may be that the ferroelectric behaviour of chiral smectic C-liquid crystal polymers will provide a mechanism for preparing stable materials. Zentel [190] has synthesized elastomers based on these materials which may have interesting applications. Le Barny and Dubois [184] discuss a few other possibilities.

3.2. *Nylons*

Lovinger [191] has pointed out that odd nylons, specifically Nylon 11, exhibit all the characteristics required to be classed as ferroelectrics. In the crystal, the structure of

which is shown schematically in figure 30, the molecules are packed in hydrogen-bonded sheets which cause the dipoles to be aligned [192]. Early studies of the poling, piezoelectric and pyroelectric properties [193–196] showed that, although the coefficients are smaller than those of PVF_2, Nylon 11 is indeed ferroelectric.

More recent studies [197–199] have shown that the coercive fields and remanent polarizations in both Nylon 11 and Nylon 7 are comparable with those in PVF_2.

4. Concluding remarks

It is now well established that some polymers are ferroelectric. PVF_2 and its copolymers with F_3E and F_4E have been subjected to fairly intensive scrutiny and it has been found that they behave very much like the more familiar ceramic ferroelectrics. The coercive field is considerably higher and the mechanisms by which the direction of polarization is changed are clearly different since the molecules are long chains of atoms covalently bonded together. The mechanical properties are very different also. PVF_2 is typically and easily prepared in thin films which are tough, strong and very flexible like many polymer films.

The major factors contributing to the piezoelectric and pyroelectric effects have been identified but many details are yet to be resolved. Studies of these phenomena in the polymeric ferroelectrics have led to new insight into physical phenomena, as is often the case in investigations of very different materials or with new experimental techniques. For example, a new type of contribution to pyroelectricity was established, reversible changes in crystallinity, and it was found, both theoretically and experimentally, that the direct and converse piezoelectric coefficients are not equal. It is generally believed that these coefficients are equal and the correction for high-modulus materials appears to be of the order of 10%, but in a low-modulus material such as PVF_2 the correction term can even be dominant.

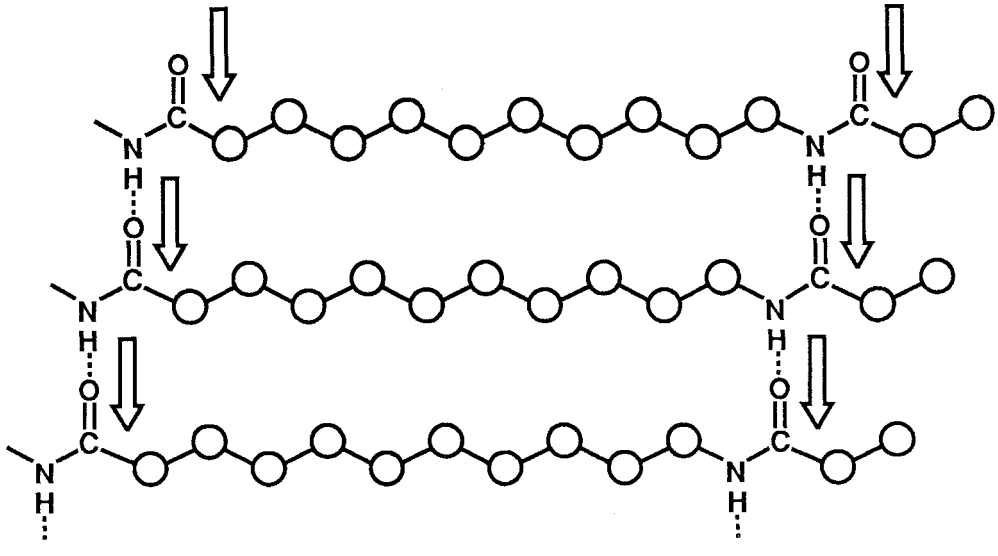

Figure 30. A schematic model of the crystal structure of Nylon 11. The circles represent methylene groups and the arrows show the orientation of the dipole moments normal to the chain axis. (From Lovinger [191].)

We have not discussed applications and refer the reader interested in this area to the book by Wang *et al.* [14]. However, a few comments may be in order. The fact that there is now a ferroelectric that is readily available as thin tough flexible films has led to some very different applications. Speakers and earphones which utilize d_{31} have been commercialized [200] and bimorphs which bend 180° in a few centimetres upon application of an electric field have been made [201]. Fans made from PVF_2 bimorphs have been proposed to cool electrical circuits [201]. The low modulus and high coercive field of PVF_2 have made it attractive as a transducer for the generation of ultrasonic waves in water [202] and it has been shown that it has very useful properties for the measurement of shock waves [72]. At Sandia National Laboratories it is now used as a standardized gauge for the measurement of stress pulses of durations up to milliseconds with a resolution of nanoseconds over a range of a few bars to at least 0·5 Mbar [203].

It is clear that ferroelectric polymers have a bright future.

Acknowledgments

Dr Andrew J. Lovinger and Dr Philip L. Taylor kindly read an early version of this review and provided useful comments. This work was performed at Sandia National Laboratories, a U.S. Department of Energy facility and was supported under Contract No. DE-AC04-76-DP00789.

References

[1] HEAVISIDE, O., 1892, *Electrical Papers*, Vol. 1 (London: Macmillan).
[2] EGUCHI, M., 1919, *Proc. Phys. Math. Soc. Japan*, **1**, 326.
[3] EGUCHI, M., 1925, *Phil. Mag.*, **49**, 178.
[4] FUKADA, E., 1968, *Ultrasonics*, **6**, 229.
[5] KAWAI, H., 1969, *Jap. J. appl. Phys.*, **8**, 975.
[6] BERGMAN, J. G., MCFEE, J. H., and CRANE, G. R., 1971, *Appl. Phys. Lett.*, **18**, 203.
[7] GLASS, A. M., MCFEE, J. H., and BERGMAN, J. G., 1971, *J. appl. Phys.*, **42**, 5219.
[8] MCFEE, J. H., BERGMAN, J. G., and CRANE, G. R., 1972, *Ferroelectrics*, **3**, 305.
[9] LANDO, J. B., OLF, H. G., and PETERLIN, A., 1966, *J. Polym. Sci.* A-1, **4**, 941.
[10] LINES, M. E., and GLASS, A. M., 1977, *Principles and Applications of Ferroelectrics and Related Materials* (Oxford: Clarendon).
[11] SESSLER, G. M., 1987, *Electrets*, Topics in Applied Physics, Vol. 33, second edition, edited by G. M. Sessler (Berlin: Springer), p. 1.
[12] NYE, J. F., 1957, *Physical Properties of Crystals* (New York: Oxford University Press).
[13] LOVINGER, A. J., 1982, *Developments in Crystalline Polymers 1*, edited by D. C. Bassett (London: Applied Science), p. 195.
[14] WANG, T. T., HERBERT, J. M., and GLASS, A. M. (editors), 1988, *The Applications of Ferroelectric Polymers* (Glasgow: Blackie).
[15] FURUKAWA, T., 1989, *IEEE Trans. Electr. Insul.*, **EI-24**, 375.
[16] FURUKAWA, T., 1989, *Phase Transitions*, **18**, 143.
[17] BROADHURST, M. G., and DAVIS, G. T., 1987, *Electrets*, Topics in Applied Physics, Vol. 33, second edition, edited by G. M. Sessler (Berlin: Springer), p. 285.
[18] DAVIS, G. T., 1988, *The Applications of Ferroelectric Polymers*, edited by T. T. Wang, J. M. Herbert and A. M. Glass (Glasgow: Blackie), p. 37.
[19] HAYAKAWA, R., and WADA, Y., 1973, *Adv. Polym. Sci.*, **11**, 1.
[20] KEPLER, R. G., and ANDERSON, R. A., 1980, *CRC Crit. Rev. Solid St. Mater. Sci.*, **9**, 399.
[21] WILSON, C. W. III, and SANTES, E. R. JR, 1965, *J. Polym. Sci.* C, **8**, 97.
[22] FARMER, B. L., HOPFINGER, A. J., and LANDO, J. B., 1972, *J. appl. Phys.*, **43**, 4293.
[23] DESANTIS, P., GIGLIO, E., LIQUORI, A. M., and RIPAMONTI, A., 1963, *J. Polym. Sci.* A, **1**, 1383.
[24] LANDO, J. B., and DOLL, W. W., 1968, *J. Macromol. Sci. Phys.*, **2**, 205.

[25] NAKAGAWA, K., and ISHIDA, Y., 1973, *J. Polym. Sci. Polym. Phys. Ed.*, **11**, 2153.
[26] LOVINGER, A. J., 1982, *Macromolecules*, **15**, 40.
[27] WEINHOLD, S., LITT, M., and LANDO, J. B., 1984, *Ferroelectrics*, **57**, 277.
[28] DOLL, W. W., and LANDO, J. B., 1970, *J. Macromol. Sci. Phys.* B, **4**, 309.
[29] HASEGAWA, R., TAKAHASHI, Y., CHATANI, Y., and TADOKORO, H., 1972, *Polym. J.*, **3**, 600.
[30] BACHMAN, M. A., and LANDO, J. B., 1981, *Macromolecules*, **14**, 40.
[31] GAL'PERIN, Y. L., STROGALIN, Y. V., and MLENIK, M. P., 1965, *Vysokomol. Soed.*, **7**, 933.
[32] DAVIS, G. T., MCKINNEY, J. E., BROADHURST, M. G., and ROTH, S. C., 1978, *J. appl. Phys.*, **49**, 4998.
[33] BACHMAN, M., GORDON, W. L., WEINHOLD, S., and LANDO, J. B., 1980, *J. appl. Phys.*, **51**, 5095.
[34] WEINHOLD, S., LITT, M. H., and LANDO, J. B., 1980, *Macromolecules*, **13**, 1178.
[35] TAKAHASHI, Y., and TADAKORO, H., 1980, *Macromolecules*, **13**, 1317.
[36] LOVINGER, A. J., 1981, *Macromolecules*, **14**, 322.
[37] SHUFORD, R. J., WILDE, A. F., RICCA, J. J., and THOMAS, G. R., 1976, *Polym. Eng. Sci.*, **16**, 25.
[38] CAIS, R. E., and KOMETANI, J. M., 1985, *Macromolecules*, **18**, 1354.
[39] LOVINGER, A. J., DAVIS, D. D., CAIS, R. E., and KOMETANI, J. M., 1987, *Polymer*, **28**, 617.
[40] OHIGASHI, H., AKAMA, S., and KOGA, K., 1988, *Jap. J. appl. Phys.*, **27**, 2144.
[41] OHIGASHI, H., and HATTORI, T., 1989, *Jap. J. appl. Phys.*, **28**, L1612.
[42] KEPLER, R. G., and ANDERSON, R. A., 1978, *J. appl. Phys.*, **49**, 1232.
[43] TAKAHASHI, N., and ODAJIMA, A., 1981, *Ferroelectrics*, **32**, 49.
[44] TAKAHASHI, Y., NAKAGAWA, Y., MIYAJI, H., and ASAI, K., 1987, *J. Polym. Sci.* C, *Polym. Lett.*, **25**, 153.
[45] BUR, A. J., BARNES, J. D., and WAHLSTRAND, K. J., 1986, *J. appl. Phys.*, **59**, 2345.
[46] SERVET, B., RIES, S., BROUSSOUX, D., and MICHERON, F., 1984, *J. appl. Phys.*, **55**, 2763.
[47] MARDIA, K. V., 1972, *Statistics of Directional Data* (New York: Academic Press), p. 122.
[48] TAMURA, M., HAGIWARA, S., MATSUMOTO, S., and ONO, N., 1977, *J. appl. Phys.*, **48**, 513.
[49] NAEGELE, D., and YOON, D. Y., 1978, *Appl. Phys. Lett.*, **33**, 132.
[50] CORTILI, G., and ZERBI, G., 1967, *Spectrochim. Acta* A, **23**, 285.
[51] KOBAYASHI, M., TASHIRO, K., and TADAKORO, H., 1975, *Macromolecules*, **8**, 158.
[52] ASLAKSEN, E. W., 1972, *J. chem. Phys.*, **57**, 2358.
[53] DVEY-AHARON, H., SLUCKIN, T. J., TAYLOR, P. L., and HOPFINGER, A. J., 1980, *Phys. Rev.* B, **21**, 3700.
[54] MCKINNEY, J. E., DAVIS, G. T., and BROADHURST, M. G., 1980, *J. appl. Phys.*, **51**, 1676.
[55] TAMURA, M., OGASAWARA, K., ONO, N., and HAGIWARA, S., 1974, *J. appl. Phys.*, **45**, 3768.
[56] KEPLER, R. G., 1978, *Org. Coatings Plast. Chem.*, **38**, 706.
[57] FURUKAWA, T., DATE, M., and FUKADA, E., 1980, *J. appl. Phys.*, **51**, 1135.
[58] DAVIS, G. T., BROADHURST, M. G., LOVINGER, A. J., and FURUKAWA, T., 1984, *Ferroelectrics*, **57**, 73.
[59] FURUKAWA, T., NAKAJIMA, K., KOIZUMI, T., and DATE, M., 1987, *Jap. J. appl. Phys.*, **26**, 1039.
[60] LUONGO, J. P., 1972, *J. Polym. Sci.* A-2, **10**, 1119.
[61] SOUTHGATE, P. D., 1976, *Appl. Phys. Lett.*, **28**, 250.
[62] LATOUR, M., 1977, *Polymer*, **18**, 278.
[63] DAS-GUPTA, D. K., and DOUGHTY, L., 1978, *J. Phys.* D, **11**, 2415.
[64] DAS-GUPTA, D. K., and DOUGHTY, L., 1977, *Appl. Phys. Lett.*, **31**, 585.
[65] SUSSNER, H., NAEGELE, D., DILLER, R. D., and YOON, D. Y., 1978, *Org. Coatings Plast. Chem.*, **38**, 266.
[66] NAEGELE, D., YOON, D. Y., and BROADHURST, M. G., 1978, *Macromolecules*, **11**, 1297.
[67] SERVET, B., and RAULT, J., 1979, *J. Phys., Paris*, **40**, 1145.
[68] DAVIES, G. R., and SINGH, H., 1979, *Polymer*, **20**, 772.
[69] DVEY-AHARON, H., TAYLOR, P. L., and HOPFINGER, A. J., 1980, *J. appl. Phys.*, **51**, 5184.
[70] LOVINGER, A. J., 1981, *Macromolecules*, **14**, 225.
[71] TAKASE, Y., SCHEINBEIM, J. I., and NEWMAN, B. A., 1989, *J. Polym. Sci.* B, *Polym. Phys.*, **27**, 2347.
[72] BAUER, F., 1983, *Ferroelectrics*, **49**, 231.
[73] TAKASE, Y., TANAKA, H., WANG, T. T., CAIS, R. E., and KOMETANI, J. M., 1987, *Macromolecules*, **20**, 2318.

[74] PAULING, L., 1948, *The Nature of the Chemical Bond*, second edition (Ithaca, New York: Cornell University Press), p. 68.
[75] BROADHURST, M. G., DAVIS, G. T., MCKINNEY, J. E., and COLLINS, R. E., 1978, *J. appl. Phys.*, **49**, 4992.
[76] ONSAGER, L., 1936, *J. Am. chem. Soc.*, **58**, 1486.
[77] KITTEL, C., 1986, *Introduction to Solid State Physics*, sixth edition (New York: Wiley), p. 366.
[78] MOPSIK, F., and BROADHURST, M. G., 1975, *J. appl. Phys.*, **46**, 4204.
[79] KAKUTANI, H., 1970, *J. Polym. Sci.* A-2, **8**, 1177.
[80] PURVIS, C. K., and TAYLOR, P. L., 1982, *Phys. Rev.* B, **26**, 4547.
[81] PURVIS, C. K., and TAYLOR, P. L., 1983, *J. appl. Phys.*, **54**, 1021.
[82] AL-JISHI, R., and TAYLOR, P. L., 1985, *J. appl. Phys.*, **57**, 897.
[83] AL-JISHI, R., and TAYLOR, P. L., 1985, *J. appl. Phys.*, **57**, 902.
[84] OGURA, H., and CHIBA, A., 1987, *Ferroelectrics*, **74**, 347.
[85] PFISTER, G., ABKOWITZ, M., and CRYSTAL, R. G., 1973, *J. appl. Phys.*, **44**, 2064.
[86] MURAYAMA, N., 1975, *J. Polym. Sci.* A-2, **13**, 929.
[87] MURAYAMA, N., OIKAWA, T., KATTO, T., and NAKAMURA, K., 1975, *J. Polym. Sci.* A-2, **13**, 1033.
[88] OSHIKI, M., and FUKADA, E., 1976, *Jap. J. Appl. Phys.*, **15**, 43.
[89] SHUFORD, R. J., WILDE, A. F., RICCA, J. J., and THOMAS, G. R., 1976, *Polym. Eng. Sci.*, **16**, 25.
[90] BLEVIN, W. R., 1977, *Appl. Phys. Lett.*, **31**, 6.
[91] BUCHMAN, P., 1973, *Ferroelectrics*, **5**, 39.
[92] HICKS, J. C., and JONES, T. E., 1981, *Ferroelectrics*, **32**, 119.
[93] FURUKAWA, T., and JOHNSON, G. E., 1981, *Appl. Phys. Lett.*, **38**, 1027.
[94] FURUKAWA, T., DATE, M., and JOHNSON, G. E., 1983, *J. appl. Phys.*, **54**, 1540.
[95] FATUZZO, E., and MERZ, W. J., 1967, *Ferroelectricity* (New York: Wiley).
[96] MERZ, W. J., 1954, *Phys. Rev.*, **95**, 690.
[97] STADLER, H. L., 1958, *J. appl. Phys.*, **29**, 1485.
[98] WIEDER, H. H., 1960, *J. appl. Phys.*, **31**, 180.
[99] CLARK, J. D., and TAYLOR, P. L., 1982, *Phys. Rev. Lett.*, **49**, 1532.
[100] SCHEINBEIM, J. I., LITT, M. H., and LANDO, J. B., 1976, unpublished results.
[101] ODAJIMA, A., WANG, T. T., and TAKASE, Y., 1985, *Ferroelectrics*, **62**, 39.
[102] AL-JISHI, R., and TAYLOR, P. L., 1987, *Ferroelectrics*, **73**, 343.
[103] TAKASE, Y., and ODAJIMA, A., 1983, *Jap. J. Appl. Phys.*, **22**, L318.
[104] TAKASE, Y., ODAJIMA, A., and WANG, T. T., 1986, *J. appl. Phys.*, **60**, 2920.
[105] FURUKAWA, T., DATE, M., OHUCHI, M., and CHIBA, A., 1984, *J. appl. Phys.*, **56**, 1481.
[106] FURUKAWA, T., MATSUZAKI, H., SHIINA, M., and TAJITSU, Y., 1985, *Jap. J. appl. Phys.*, **24**, L661.
[107] LOVINGER, A. J., DAVIS, G. T., FURUKAWA, T., and BROADHURST, M. G., 1982, *Macromolecules*, **15**, 323.
[108] TASHIRO, K., TAKANO, K., KOBAYASHI, M., CHATANI, Y., and TADOKORO, H., 1984, *Ferroelectrics*, **57**, 297.
[109] KIMURA, K., and OHIGASHI, H., 1983, *Appl. Phys. Lett.*, **43**, 834.
[110] KIMURA, K., and OHIGASHI, H., 1986, *Jap. J. appl. Phys.*, **25**, 383.
[111] KEPLER, R. G., and ANDERSON, R. A., 1979, unpublished results.
[112] YAGI, T., 1979, *Polym. J.*, **11**, 353.
[113] YAGI, T., and TATEMOTO, M., 1979, *Polym. J.*, **11**, 429.
[114] YAGI, T., 1979, *Polym. J.*, **11**, 711.
[115] YAGI, T., TATEMOTO, M., and SAKO, J.-I., 1980, *Polym. J.*, **12**, 209.
[116] HIGASHIHATA, Y., SAKO, J., and YAGI, T., 1981, *Ferroelectrics*, **32**, 85.
[117] KITAYAMA, T., UEDA, T., and YAMADA, T., 1980, *Ferroelectrics*, **28**, 301.
[118] YAMADA, T., UEDA, T., and KITAYAMA, T., 1981, *J. appl. Phys.*, **52**, 948.
[119] UCHIDOI, M., IWAMA, T., IWAMA, K., and TAMURA, M., 1979, *Rep. Prog. Polym. Phys. Jpn.*, **22**, 345.
[120] TAJITSU, Y., CHIBA, A., FURUKAWA, T., DATE, M., and FUKADA, E., 1980, *Appl. Phys. Lett.*, **36**, 286.
[121] FURUKAWA, T., JOHNSON, G. E., BAIR, H. E., TAJITSU, Y., CHIBA, A., and FUKADA, E., 1981, *Ferroelectrics*, **32**, 61.

[122] TASHIRO, K., TAKANO, K., KOBAYASHI, M., CHATANI, Y., and TADOKORO, H., 1981, *Polymer*, **22,** 1312.
[123] FURUKAWA, T., and JOHNSON, G. E., 1981, *J. appl. Phys.*, **52,** 940.
[124] DAVIS, G. T., FURUKAWA, T., LOVINGER, A. J., and BROADHURST, M. G., 1982, *Macromolecules*, **15,** 329.
[125] KOLDA, R. R., and LANDO, J. B., 1975, *J. Macromol. Sci. Phys.* B, **11,** 21.
[126] LOVINGER, A. J., FURUKAWA, T., DAVIS, G. T., and BROADHURST, M. G., 1983, *Ferroelectrics*, **50,** 553.
[127] LOVINGER, A. J., FURUKAWA, T., DAVIS, G. T., and BROADHURST, M. G., 1983, *Polymer*, **24,** 1233.
[128] KOIZUMI, N., MURATA, Y., and HAIKAWA, N., 1985, *Jap. J. appl. Phys. Suppl. 2*, **24,** 862.
[129] TASHIRO, K., and KOBAYASHI, M., 1985, *Jap. J. appl. Phys., Suppl. 2*, **24,** 873.
[130] GREEN, J. S., RABE, J. P., and RABOLT, J. F., 1986, *Macromolecules*, **19,** 1725.
[131] TASHIRO, K., and KOBAYASHI, M., 1989, *Phase Transitions*, **18,** 213.
[132] LOVINGER, A. J., 1983, *Macromolecules*, **16,** 1529.
[133] LOVINGER, A. J., JOHNSON, G. E., BAIR, H. E., and ANDERSON, E. W., 1984, *J. appl. Phys.*, **56,** 2412.
[134] LOVINGER, A. J., DAVIS, D. D., CAIS, R. E., and KOMETANI, J. M., 1986, *Macromolecules*, **19,** 1491.
[135] LOVINGER, A. J., DAVIS, D. D., CAIS, R. E., and KOMETANI, J. M., 1988, *Macromolecules*, **21,** 78.
[136] ANDERSON, R. A., and KEPLER, R. G., 1981, *Ferroelectrics*, **32,** 13.
[137] ZHELUDEV, I. S., 1971, *Physics of Crystalline Dielectrics*, Vol. 2 (New York: Plenum), p. 553.
[138] DVEY-AHARON, H., and TAYLOR, P. L., 1981, *Ferroelectrics*, **33,** 103.
[139] BURKARD, H., and PFISTER, G., 1974, *J. appl. Phys.*, **45,** 3360.
[140] KEPLER, R. G., and ANDERSON, R. A., 1978, *J. appl. Phys.*, **49,** 4490.
[141] DATE, M., 1986, *IEEE Trans. Electr. Insul.*, **EI-21,** 539.
[142] FURUKAWA, T., and WANG, T. T., 1988, *The Applications of Ferroelectric Polymers*, edited by T. T. Wang, J. M. Herbert and A. M. Glass (Glasgow: Blackie), p. 66.
[143] KEPLER, R. G., and ANDERSON, R. A., 1978, *J. appl. Phys.*, **49,** 4918.
[144] KEPLER, R. G., and ANDERSON, R. A., 1984, *Molec. Cryst. Liq. Cryst.*, **106,** 345.
[145] KAVESH, S., and SCHULTZ, J. M., 1970, *J. Polym. Sci.* A-2, **8,** 243.
[146] NIX, E. L., NANAYAKKARA, J., DAVIES, G. R., and WARD, I. M., 1988, *J. Polym. Sci.* B, *Polym. Phys.*, **26,** 127.
[147] SCHULTZ, J. M., LIN, J. S., HENDRICKS, R. W., LAGASSE, R. R., and KEPLER, R. G., 1980, *J. appl. Phys.*, **51,** 5508.
[148] ANDERSON, R. A., KEPLER, R. G., and LAGASSE, R. R., 1981, *Ferroelectrics*, **33,** 91.
[149] KEPLER, R. G., ANDERSON, R. A., and LAGASSE, R. R., 1982, *Phys. Rev. Lett.*, **48,** 1274.
[150] KEPLER, R. G., ANDERSON, R. A., and LAGASSE, R. R., 1984, *Ferroelectrics*, **57,** 151.
[151] CALLEN, H. B., 1960, *Thermodynamics* (New York: Wiley), p. 243.
[152] CLEMENTS, J., DAVIES, G. R., and WARD, I. M., 1985, *Polymer.*, **26,** 208.
[153] DVEY-AHARON, H., SLUCKIN, T. J., and TAYLOR, P. L., 1981, *Ferroelectrics*, **32,** 25.
[154] HAYAKAWA, R., and WADA, Y., 1976, *Rep. Prog. Polym. Phys. Jpn*, **19,** 321.
[155] WADA, Y., 1976, *Jap. J. appl. Phys.*, **15,** 2041.
[156] WADA, Y., 1982, *Electronic Properties of Polymers*, edited by J. Mort and G. Pfister (New York: Wiley), p. 109.
[157] BROADHURST, M. G., MALMBERG, C. G., MOPSIK, F. I., and HARRIS, W. P., 1973, *Electrets, Charge Storage and Transport in Dielectrics*, edited by M. M. Perlman (Princeton, New Jersey: Electrochemical Society), p. 492.
[158] PURVIS, C. K., and TAYLOR, P. L., 1982, *Phys. Rev.* B, **26,** 4564.
[159] OHIGASHI, H., 1976, *J. appl. Phys.*, **47,** 949.
[160] FUKADA, E., DATE, M., and HARA, K., 1969, *Jap. J. appl. Phys.*, **8,** 151.
[161] BUI, L. N., SHAW, H. J., and ZITELLI, L. T., 1977, *IEEE Trans. Sonics Ultrasonics*, **SU-24,** 331.
[162] SCHEWE, H., 1982, *Ultrasonics Symposium Proceedings*, edited by B. R. McAvoy (New York: IEEE), p. 519.
[163] REZVANI, B., and LINVILL, J. G., 1979, *Appl. Phys. Lett.*, **34,** 828.
[164] NIX, E. L., and WARD, I. M., 1986, *Ferroelectrics*, **67,** 137.

[165] *IEEE Standard on Piezoelectricity*, 1987, ANSI–IEEE Standard No. 176-1987 (New York: Institute of Electrical and Electronic Engineers).
[166] BROSSAT, T., BICHON, G., LEMONON, C., ROYER, M., and MICHERON, F., 1979, *C. r. hebd. Séanc. Acad. Sci., Paris*, B, **288,** 53.
[167] HUMPHREYS, J., WARD, I. M., MCGRATH, J. C., and NIX, E. L., 1986, *Ferroelectrics*, **67,** 131.
[168] HUMPHREYS, J., LEWIS, E. L. V., WARD, I. M., NIX, E. L., and MCGRATH, J. C., 1988, *J. Polym. Sci.* B, *Polym. Phys.*, **26,** 141.
[169] WANG, T. T., 1979, *J. appl. Phys.*, **50,** 6091.
[170] YAGI, T., HIGASHIHATA, Y., KUKUYAMA, K., and SAKO, J., 1984, *Ferroelectrics*, **57,** 327.
[171] FURUKAWA, T., WEN, J. X., SUZUKI, K., TAKASHINA, Y., and DATE, M., 1984, *J. appl. Phys.*, **56,** 829.
[172] FURUKAWA, T., and WEN, J. X., 1984, *Jap. J. appl. Phys.*, **23,** L677.
[173] FUKADA, E., and TAKASHITA, S., 1969, *Jap. J. appl. Phys.*, **8,** 960.
[174] FUKADA, E., and SAKURAI, T., 1971, *Polym. J.*, **2,** 656.
[175] FURUKAWA, T., AIBA, J., and FUKADA, E., 1979, *J. appl. Phys.*, **50,** 3615.
[176] TASHIRO, M., KOBAYASHI, M., TASOKORO, H., and FUKADA, E., 1980, *Macromolecules*, **13,** 691.
[177] WADA, Y., and HAYAKAWA, R., 1981, *Ferroelectrics*, **32,** 115.
[178] SATO, H., and GAMO, H., 1986, *Jap. J. appl. Phys.*, **25,** L990.
[179] WICKER, A., BERGE, B., LAJZEROWICZ, J., and LEGRAND, J. F., 1989, *Ferroelectrics*, **92,** 35.
[180] MEYER, R. B., LIEBERT, L., STRZELECKI, L., and KELLER, P., 1975, *J. Phys. Lett.*, **36,** L69.
[181] CLARK, N., and LAGERWALL, S., 1980, *Appl. Phys. Lett.*, **36,** 899.
[182] SHIBEAV, V., KOSLOVSKY, M., BERESNEV, L., BLINOV, L., and PLATE, N., 1984, *Polym. Bull.*, **12,** 299.
[183] SHIBAEV, V., and PLATE, N., 1985, *Pure Appl. Chem.*, **57,** 1589.
[184] LE BARNY, P., and DUBOIS, J. C., 1989, *Side Chain Liquid Crystal Polymers*, edited by C. B. McArdle (London: Blackie), p. 130.
[185] BLINOV, L., BAILKALOV, V., BARNIK, M., BERESNEV, L., POZHIDAYEV, E., and YABLONSKY, S., 1987, *Liq. Cryst.*, **2,** 121.
[186] SCHEROWSKY, G., SCHLIWA, A., SPRINGER, J., KUEHNPAST, K., and TRAPP, W., 1989, *Liq. Cryst.*, **5,** 1281.
[187] SKARP, K., and HANDSCHY, M. A., 1988, *Mol. Cryst. Liq. Cryst*, **165,** 439.
[188] KAPITZA, H., ZENTEL, R., TWIEG, R. J., NGUYEN, C., VALLERIEN, S. U., KREMER, F., and WILLSON, C. G., 1990, *Adv. Mater.*, **2,** 539.
[189] VALLERIEN, S. U., ZENTEL, R., KREMER, F., KAPITZA, H., and FISCHER, E. W., 1989, *Makromol. Chem., Rapid Commun.*, **10,** 333.
[190] ZENTEL, R., 1989, *Adv. Mater.*, **28,** 1407.
[191] LOVINGER, A. J., 1985, *Jap. J. appl. Phys., Suppl. 2*, **24,** 18.
[192] SLICHTER, W. P., 1959, *J. Polym. Sci.*, **36,** 259.
[193] LITT, M. H., HSU, C., and BASU, P., 1977, *J. appl. Phys.*, **48,** 2208.
[194] NEWMAN, B. A., CHEN, P., PAE, K. D., and SCHEINBEIM, J. I., 1980, *J. appl. Phys.*, **51,** 5161.
[195] GELFANDBEIN, V., and KATZ, D., 1981, *Ferroelectrics*, **33,** 111.
[196] MATHUR, S. C., SCHEINBEIM, J. I., and NEWMAN, B. A., 1984, *J. appl. Phys.*, **56,** 2419.
[197] LEE, J. W., TAKASE, Y., NEWMAN, B. A., and SCHEINBEIM, J. I., 1991, *J. Polym. Sci.* B, *Polym. Phys.*, **29,** 273.
[198] LEE, J. W., TAKASE, Y., NEWMAN, B. A., and SCHEINBEIM, J. I., 1991, *J. Polym. Sci.* B, *Polym. Phys.*, **29,** 279.
[199] TAKASE, Y., LEE, J. W., SCHEINBEIM, J. I., and NEWMAN, B. A., 1991, *Macromolecules* (submitted).
[200] TAMURA, M., YAMAGUCHI, T., OYABA, T., and YOSHIMI, T., 1975, *J. Audio Eng. Soc.*, **23,** 21.
[201] TODA, M., 1981, *Ferroelectrics*, **32,** 127.
[202] BUI, L., SHAW, H. J., and ZITELLI, L. T., 1976, *Electron Lett.*, **12,** 393.
[203] REED, R. P., and GREENWOLL, J. I., 1988, Report No. SAND88-2907 (Sandia National Laboratories).
[204] LOVINGER, A. J., 1983, *Science*, **220,** 1115.
[205] WALBA, D. M., and CLARK, N. A., 1987, *Spatial Light Modulators and Applications II*, Proceedings of the SPIE, Vol. 825 (Bellingham, Washington: SPIE), p. 81.